UNIVERSIDADE DA BEIRA INTERIOR
Ciências

Production of membranes for filtration of biomolecules

Pedro Henrique Barata Castilho

Dissertação para obtenção do Grau de Mestre em
Biotecnologia
(2º ciclo de estudos)

Orientador: Prof. Doutor António Miguel Parreira Cabral Forjaz Morão
Co-orientador: Prof. Doutor Ilídio Joaquim Sobreira Correia

Covilhã, Outubro de 2014

UNIVERSIDADE DA BEIRA INTERIOR
Ciências

Produção de membranas para filtração de biomoléculas

Pedro Henrique Barata Castilho

Dissertação para obtenção do Grau de Mestre em
Biotecnologia
(2º ciclo de estudos)

Orientador: Prof. Doutor António Miguel Parreira Cabral Forjaz Morão
Co-orientador: Prof. Doutor Ilídio Joaquim Sobreira Correia

Covilhã, Outubro de 2014

List of Publications

- Article published in peer reviewed international scientific journal:

Correia, T.R., B.P. Antunes, P.H. Castilho, J.C. Nunes, M.T. Pessoa de Amorim, I.C. Escobar, J.A. Queiroz, I.J. Correia, and A.M. Morão, *A bi-layer electrospun nanofiber membrane for plasmid DNA recovery from fermentation broths*. Separation and Purification Technology, 2013. 112: p. 20-25.

- Article submitted in peer reviewed in international scientific journal:

Pedro H. Castilho, Tiago R. Correia, Maria T. Pessoa de Amorim, Isabel C. Escobar, João A. Queiroz, Ilídio J. Correia, António M. Morão, *Modification of microfiltration membranes by hydrogel impregnation for pDNA purification.* Journal of Applied Polymer Science, 2014.

- Poster communications:

Correia, T.R., B.P. Antunes, P.H. Castilho, J.C. Nunes, M.T. Pessoa de Amorim, I.C. Escobar, J.A. Queiroz, I.J. Correia, and A.M. Morão, *A bi-layer electrospun nanofiber membrane for plasmid DNA recovery from fermentation broths*. VIII Annual CICS Symposium, 1-2 de Julho de 2013, Faculdade de Ciências da Saúde, Universidade da Beira Interior, Covilhã, Portugal.

Correia T.R., Antunes B.P., Castilho P.H., Nunes J.C., de Amorim M.T.P., Escobar I.C., Queiroz J.A., Correia I.J., Morão A.M.; "A bi-layer electrospun nanofiber membrane for plasmid DNA recovery from fermentation broths"; Encontro Bienal das Divisões Técnicas da Sociedade Portuguesa dos Materiais, Universidade da Beira Interior, Covilhã, Portugal 21 de Maio de 2014.

Acknowledgments

This year was laborious and scientifically rewarding. Nevertheless, this task was carried out with the help of some people who I want to thank:

Firstly, I would like to express my gratitude to my supervisor Professor Miguel Morão for his guidance, patience and support during this work plan development. I would also like to thank him for all the conditions and knowledge provided to me that allow me to develop the work presented in this thesis.

Likewise, I would like to thank my co-supervisor, Professor Ilídio Correia, for the teachings, guidance and relevant suggestions that he made at a first stage of the work.

Furthermore, I would like to thank to my dear colleague Sónia Miguel from University of Beira Interior for the help in the acquisition of scanning electron microscopy images and energy dispersive spectra of the produced membranes, as well as to José Nunes for all his help and useful advices in what concerns the filtration process and to Sónia Sousa by the measurements of the contact angles.

I also acknowledge my work group for creating a healthy work environment, and for offering me support and kindness in the toughest moments.

To my closest friends I would like to express my deepest gratitude, for being at my side in the difficult times, as well as in the happiest ones.

I thank to my girlfriend for the patience and comprehension that she had with me, and for being at my side in the darkest days, as well as in the joyful ones.

Definitely, to my parents and brother, who have been supporting me for all these years. I deeply want to thank them for their unconditional faith, guidance and love. I thank you from the bottom of my heart.

Last, but not least, to my grandfather Joaquim Penedo Churro, that is no longer present but who taught me to be who I am today. This thesis is dedicated to you.

"Filho, há sempre alguma coisa que fazer!"

Joaquim Penedo Churro

Abstract

Plasmids are autonomously replicating entities that can be found in all bacterial species and contribute for bacterial adaption and evolution. The demand of highly purified biomolecules has triggered the development of new separation technologies. Herein, plasmid DNA (pDNA) purification process has been extensively investigated, in order to obtain highly purified molecules for gene therapy applications and DNA (deoxyribonucleic acid) vaccines. The purification of plasmid DNA is currently performed by different techniques, namely chromatography (anion-exchange, hydrophobic interaction, reversed phase, affinity and size-exclusion), enzymatic and membrane processes. Membrane technology is a broad and highly interdisciplinary field, where process engineering, material science and chemistry meet to produce membranes that have a wide range of applications, such as water, biomolecules and plasmid DNA purification. Furthermore, membrane systems take advantage of their selectivity, high surface-area-per-unit-volume. Herein, the main goal was to produce membrane systems - electrospinning membranes: poly *ε*-caprolactone, polyethylene oxide and *k*-carrageenan; modified-*nylon* membranes: *nylon* membrane impregnated with agarose - in order to perform microfiltration and ultrafiltration processes, respectively. The produced membranes were characterized by Scanning Electron Microscopy, Attenuated Total Reflectance-Fourier Transform Infrared Spectroscopy and Energy Dispersive Spectroscopy. The water contact angles were also determined and the results obtained showed that the produced membranes presented a hydrophilic character, which is in agreement with the date previously described in literature. Porosity studies were also performed and the results demonstrated that the electrospun membranes have porosity around to 80% and the modified-*nylon* membranes have porosities of approximately 40%. These values can be considered to be very high, when comparing these membranes to conventional microfiltration and ultrafiltration membranes produced by phase inversion. The plasmid DNA rejection was determined on the membranes produced and the experimental results showed that the modified-*nylon* membrane presented rejection values up to 100%, depending on the imposed permeate flux, which is an attractive feature for its application on plasmid DNA purification by ultrafiltration. In respect to the electrospun membranes produced the observed rejections were found to be lower, up to 30%, which demonstrates that this membranes need to be optimized or modified (post-synthesis modification).

Keywords

Biomolecules, electrospinning, membrane modification, microfiltration, plasmid DNA, purification, ultrafiltration.

Resumo

Os plasmídeos são entidades auto-replicantes que podem ser encontrados em todas as espécies de bactérias e que têm um papel fundamental na adaptação e evolução das bactérias. A necessidade de obter biomoléculas com um elevado grau de pureza desencadeou o desenvolvimento de novas técnicas de separação. Os processos de optimização da purificação de ADN plasmídico têm sido estudados exaustivamente, para que estes possam ser usados em aplicações de terapia génica ou em vacinas de ADN (ácido desoxirribonucleico). A purificação do ADN plasmídico tem sido realizada usando, nomeadamente a tecnologia de membranas. A tecnologia de membranas abrange uma vasta área do conhecimento, altamente interdisciplinar, onde engenharia de processos, a ciência dos materiais e a química permitem a produção de membranas aplicadas em diferentes áreas, tais como purificação de águas, biomoléculas e de ADN plasmídico, entre muitas outras. Os sistemas de separação com membranas caracterizam-se por oferecer geralmente elevada selectividade nas separações, elevadas áreas superficiais por unidade de volume do equipamento; e oferecem a possibilidade de controlar o nível de contacto e/ou mistura entre duas fases. O presente estudo teve como objectivo produzir membranas de micro e ultrafiltração para purificação de ADN plasmídico - membranas de *electrospinning*: poli *ε*-caprolactona, óxido de polietileno e *k*-carragenano; membranas de *nylon* modificadas: membrana *nylon* impregnada com agarose. As membranas produzidas foram caracterizadas por Microscopia Electrónica de Varrimento, Espectroscopia de Infravermelho com Transformada de Fourier Atenuada e Espectroscopia de Raio X por Dispersão de Energia. Os ângulos de contacto com água também foram determinados e os resultados obtidos mostraram que as membranas produzidas apresentam caracter hidrofílico. Estudos de porosidade foram igualmente efectuados e os resultados demonstraram que as membranas produzidas por *electrospinning* têm porosidades próximas de 80% e a membrana de *nylon* modificada tem uma porosidade próxima de 40%. Estes valores podem ser considerados bastante elevados, se os compararmos com valores típicos de membranas de microfiltração e ultrafiltração convencionais, produzidas por inversão de fase. A rejeição de ADN plasmídico foi determinada para ambas as membranas. Os valores obtidos mostraram que a membrana de *nylon* modificada apresentou valores de rejeição até 100%, dependendo do fluxo de permeação imposto, o que é uma característica promissora para a sua aplicação em purificação de ADN plasmídico por ultrafiltração. Relativamente às membranas produzidas por electrospinning a rejeição foi menor, apenas até 30%, o que demonstra que estas membranas precisam ser optimizadas ou eventualmente modificadas (modificação por síntese).

Palavras-chave

ADN plasmídico, biomoléculas, *electrospinning*, microfiltração, modificação de membranas, purificação, ultrafiltração.

Resumo Alargado

Os plasmídeos são entidades auto-replicantes que podem ser encontrados em todas as espécies de bactérias e que têm um papel fundamental na adaptação e evolução das bactérias. Além disso, os plasmídeos são estudados devido às suas propriedades intrínsecas, o que os torna importantes ferramentas nos estudos de biologia molecular. Os processos de optimização do ADN plasmídico têm sido estudados exaustivamente, para que estes possam ser usados em aplicações de terapia génica ou em vacinas de ADN (ácido desoxirribonucleico). A necessidade de obter biomoléculas com um elevado grau de pureza desencadeou o desenvolvimento de novas técnicas de separação. A evolução da terapia génica alcançou um importante marco histórico, nomeadamente, a autorização da EMA (European Medicines Agency) para a comercialização de um fármaco de terapia génica para o tratamento da deficiência da lipoproteína lipase. A purificação do ADN plasmídico tem sido realizada usando várias técnicas, tais como, cromatografia (troca iónica, interacção hidrofóbica, fase reversa, afinidade e exclusão molecular), enzimática e processos de membrana. Nos processos reportados na literatura, os plasmídeos são produzidos por via fermentativa e subsequente processo de purificação; este divide-se em três etapas: recuperação primária, recuperação intermediária e purificação final. A tecnologia de membranas abrange uma vasta área do conhecimento, altamente interdisciplinar, onde engenharia de processos, a ciência dos materiais e a química permitem a produção de membranas aplicadas em diferentes áreas, tais como purificação de ADN plasmídico. Os sistemas de filtração com membranas são apropriados para o processamento de moléculas biológicas, uma vez que operam, relativamente, a baixas temperaturas e pressões e não envolvem mudanças de fases, minimizando o grau de desnaturação, desactivação e/ou degradação dos produtos biológicos; além disso, não requerem o consumo de grandes quantidades de agentes químicos, por se tratar de processos puramente físicos. A filtração com membranas tem também normalmente baixos custos operatórios comparando com outros processos alternativos. Além disso, a filtração com membranas permite elevadas selectividades e elevada produtividade, sendo os sistemas bastante compactos, dada a elevada área superficial por unidade de volume dos módulos industriais. Os processos de filtração com membranas podem ser classificados tendo em conta diferentes características das membranas, nomeadamente o tamanho do poro, tamanho e carga das partículas ou moléculas retidas e a pressão exercida na membrana. Esta classificação permite distinguir as membranas de microfiltração, ultrafiltração, nanofiltração e osmose reversa. No caso da microfiltração e ultrafiltração a separação molecular é baseada essencialmente nas diferenças de tamanho das moléculas, forma e diferenças de flexibilidade estrutural. O *electrospinning* é um método fácil e barato de produzir materiais nanofibrosos. A simplicidade deste processo e a vasta gama de aplicações encontrada, incluindo engenharia de tecidos, sensores e biossensores e filtração são importantes factores que levam a um interesse progressivo no desenvolvimento de novos tipos

de membranas nanofibrosas produzidas por *electrospinning*. Este tipo de membranas oferece um conjunto de vantagens na filtração, principalmente pela elevada porosidade das membranas (tipicamente à volta de 80%) e a elevada razão de área de superfície/volume (devido à elevada área superficial das fibras), quando comparados com membranas poliméricas convencionais obtidas por inversão de fase e membranas cerâmicas. A elevada porosidade pode melhorar directamente o fluxo sem prejudicar a taxa de rejeição dos contaminantes e a elevada razão área/volume permite tirar partido de possíveis interacções físicas soluto/membrana que possam ser úteis nas separações e/ou no controlo da colmatação. Actualmente existem várias membranas de ultrafiltração disponíveis no mercado que podem ser usadas para a purificação de ADN plasmídico. Tendo em conta o tamanho das moléculas do ADN plasmídico, a modificação da superfície de membranas de microfiltração aparece como uma possível alternativa, oferecendo a possibilidade de ajustar a selectividade desejada a um caso particular. Vários estudos têm demonstrado que as propriedades da membrana, tais como resistência às proteínas, biocompatibilidade, carga e hidrofobicidade, podem ser melhoradas através de processos de modificação da superfície. No presente estudo pretendeu-se produzir membranas de microfiltração e de ultrafiltração para purificação de ADN plasmídico - membranas produzidas por *electrospinning*: poli *ε*-caprolactona, óxido de polietileno e *k*-carragenano; membranas de *nylon* modificadas: membranas de *nylon* impregnadas com agarose. As membranas produzidas foram caracterizadas por Microscopia Electrónica de Varrimento, Espectroscopia de Infravermelho com Transformada de Fourier Atenuada, Espectroscopia de Raio X por Dispersão de Energia. Os ângulos de contacto com água também foram determinados e os resultados obtidos mostraram que as membranas produzidas apresentavam caracter hidrofílico. Estudos de porosidade foram igualmente efectuados e os resultados demonstraram que as membranas produzidas por *electrospinning* têm porosidades próximas de 80% e a membrana de *nylon* modificada tem uma porosidade próxima de 40%. Estes valores podem ser considerados bastante elevados, se os compararmos com valores típicos de membranas de microfiltração e ultrafiltração convencionais, produzidas por inversão de fase. A rejeição de ADN plasmídico foi determinada para ambas as membranas. Os valores obtidos mostraram que a membrana de *nylon* modificada apresentou valores de rejeição até 100%, dependendo do fluxo de permeação imposto, o que é uma característica promissora para a sua aplicação em purificação de ADN plasmídico por ultrafiltração. Relativamente às membranas produzidas por electrospinning a rejeição foi menor, apenas até 30%, o que demonstra que estas membranas precisam ser optimizadas ou eventualmente modificadas (modificação pós-síntese).

Palavras-chave

ADN plasmídico, biomoléculas, *electrospinning*, microfiltração, modificação de membranas, purificação, ultrafiltração.

Table of Contents

List of Figures

List of Tables

List of Acronyms

ADN	Ácido Desoxirribonucleico
ARN	Ácido Ribonucleico
ATR-FTIR	Attenuated Total Reflectance-Fourier Transform Infrared Spectroscopy
BSA	Bovine Serum Albumin
DNA	Deoxyribonucleic Acid
D_s	Diffusion coefficient
ECM	Extracellular Matrix
EDTA	Ethylenediamine tetra acetic acid
EDS	Energy Dispersive Spectroscopy
EMA	European Medicines Agency
ENM	Electrospun Nanofibre Membrane
ENMC	Coated Electrospun Nanofibre Membrane
FDA	Food and Drug Administration
J_v	Flux
L_p	Hydraulic Permeability
MF	Microfiltration
MW	Molecular Weight
NF	Nanofiltration
P	Pressure
PCL	Poly ε-Caprolactone
pDNA	Plasmid DNA
PEO	Polyethylene Oxide
R_g	Radius of gyration
R_m	Molecular radius
RNA	Ribonucleic Acid
RNase	Ribonuclease

RO	Reverse Osmosis
R_{obs}	Observed rejection
R_p	Pore radius
R_s	Hydrodynamic radius
RT	Room Temperature
SDS	Sodium dodecyl sulphate
SEM	Scanning Electron Microscopy
SPM	Symmetric Pore Model
Tris-HCl	Tris(hydroxymethyl)amino methane-Hydrochloric acid
UF	Ultrafiltration

Chapter I

Introduction

1. Introduction

1.1 Plasmid DNA

Plasmids are autonomously replicating entities which can be found essentially in all bacterial species and that play a significant role in bacterial adaptation and evolution [1]. Like chromosomes, plasmids code for ribonucleic acid (RNA) molecules and proteins, replicate as cell grows and equal numbers are normally distributed to the two daughter cells upon cell division [1]. Plasmids are studied due to their intrinsic properties and serve as important tools in molecular biology studies [1], for instance, they have been used as vectors for gene therapy or vaccination in the last two decades [2-4]. The injection of plasmid DNA (pDNA) containing selected genes from pathogens can induce a protective immune response [5]. In previous studies it has been demonstrated that pDNA vaccines can simulate intracellular pathogen gene expression pathways, but are quiet safe due to a lack genetic integration, *i.e*. the injected foreign genetic material will not be integrated in the host genetic material and, therefore, it will not be responsible for an immune response in the host [6, 7].

The demand of highly purified biomolecules has triggered the development of new separation technologies. Herein, the plasmid DNA purification has been extensively investigated, in order to obtain a highly purified molecules for gene therapy applications and deoxyribonucleic acid (DNA) vaccines [8]. The evolution of gene therapy achieved an important landmark, namely, the authorization of the European Medicines Agency (EMA) for the commercialisation, in the European Union, of *Glybera* (alipogene tiparvovec) for gene therapy, to treat the lipoprotein lipase deficiency [9]. In literature there are different studies focused on this topic [1, 9-11] and the formulation of DNA vaccines [12-14] has the encouraging results shown in autoimmune diseases such as AIDS, and due to the other infectious diseases, such as hepatitis B and C, and tuberculosis [6, 7].

1.1.2 Purification methods

The final pDNA solution must strictly obey to the safety regulations imposed by the Food and Drug Administration (FDA) and/or EMA, known as Good Manufacture Products (GMP) [6]. They establish thresholds for the presence of contaminants, including harmful chemicals (cesium chloride, ethidium bromide, isopropanol, phenol or chloroform) and enzymes (RNase A, lysozyme and proteinase K), which are used in laboratory protocols and are considered unsafe or impractical, when inserted into large scale operations [15-18].

The purification of pDNA has been achieved through the use of different techniques, including chromatography (anion-exchange, hydrophobic interaction, reversed phase, affinity and size-

exclusion), enzymatic and membrane processes [19-23]. Figure 1 shows a scheme of pDNA purification process adapted from Prazeres *et al* [19], in which the authors refer the main steps of pDNA purification process, from cell lysis to the final product purification and formulation, dividing it into three stages: primary recovery, intermediate recovery and final purification. It also can be seen in Figure 1 that microfiltration (MF) and ultrafiltration (UF) can be used in most of the different phases of the process.

Primary recovery essentially consists in cell harvesting, cell disruption and the removal of cell debris from the main stream. In the intermediate recovery a more thorough purification is performed, removing genomic DNA, RNA, proteins, endotoxins and concentrating the pDNA. The final purification is the most important step, because it leads to a pure pDNA, free of contaminants; in this step the remains of genomic DNA, RNA, proteins, endotoxins, undesirable plasmid isoforms, salts and process contaminants are removed. All this steps are resumed in Figure 1.

On a large scale, it is of paramount importance to develop a set of highly efficient processes, since the conventional laboratory pDNA purification procedures, as already described, are quite complex to scale up and involve the use of chemicals that are forbidden by regulatory agencies [19]. Hereupon, purification processes that use membranes were found as a good solution for purify pDNA in larger scale, since they avoid the use of dangerous chemicals [15, 20, 23]. Furthermore, MF and UF membranes avoid precipitation solvents and centrifugation steps. However, the pDNA purification from RNA by ultrafiltration remains a challenge as recently has been published in the literature [15, 23].

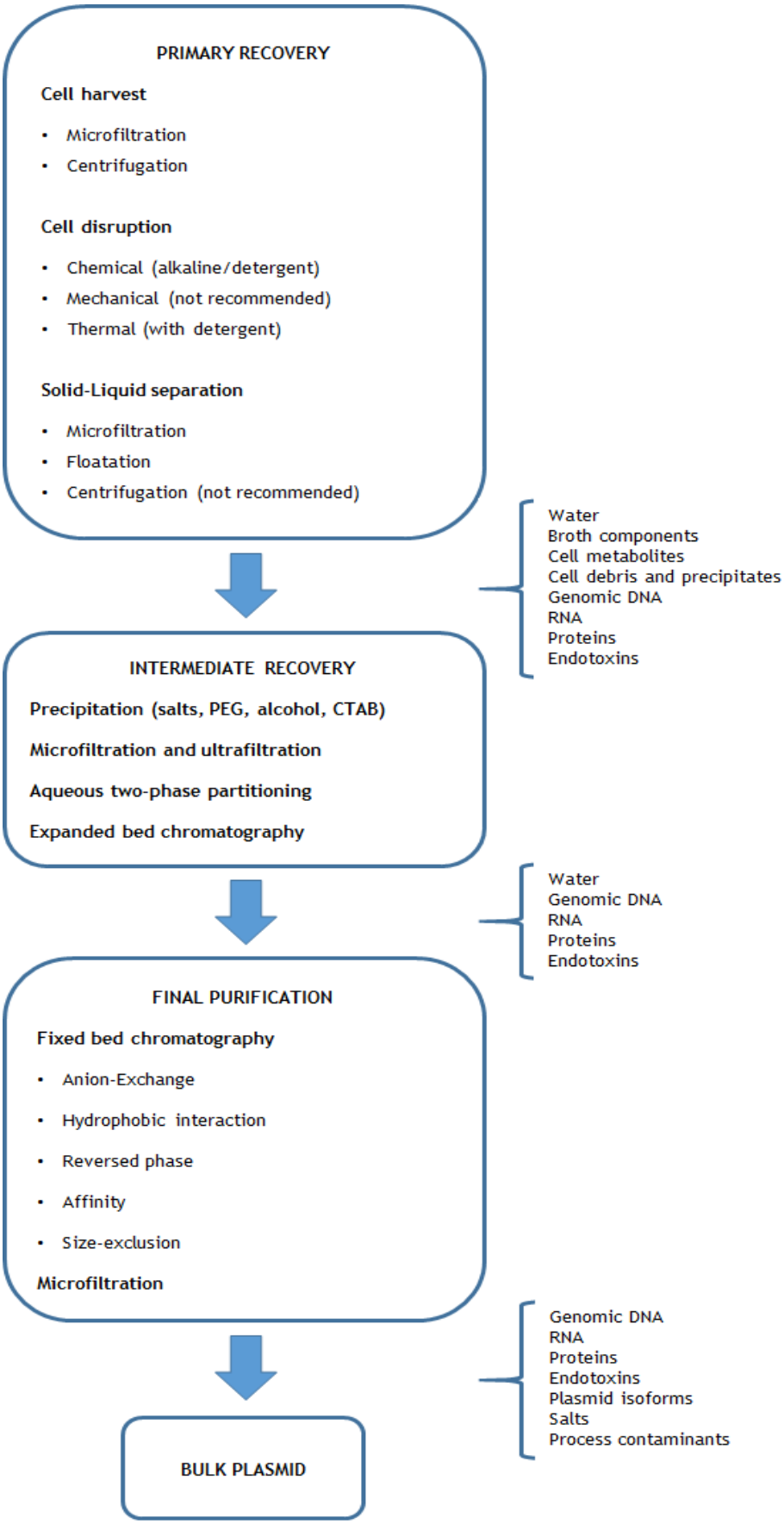

Figure 1 Representation of the downstream process used for the production of purified pDNA (adapted from [19]).

1.2 Membrane technology

Membrane technology is a broad and highly interdisciplinary field, where process engineering, material science and chemistry meet to produce membranes that have a wide range of applications [24]. Membrane filtration usually operates under mild conditions and does not require the addition of chemicals to be performed, thus making it generally well-suitable for processing of biotechnology products. Membrane filtration also has lower operation costs than alternative processes like chromatography and precipitation [25], and a reduced environmental impact. Moreover, they possess characteristics that enable a linear scale-up of the process and allow its easy automation. Membrane filtration processes can be also designed for operating in continuous mode [26-28].

Membrane filtration systems take advantage of their high selectivity and high surface-area-per-unit-volume [29]. They are suitable for processing biological molecules since they operate at relatively low temperatures and pressures and involve no phase changes or chemical additives, thereby minimizing the extent of denaturation, deactivation, and/or degradation of biological products [29]. Membrane processes usually achieve high efficiency in terms of separation, which has a great economic impact [30].

1.2.1 Membrane classification

Membrane processes can be sorted by several criteria, distinguishing microfiltration from ultrafiltration, nanofiltration and from reverse osmosis. Those criteria are: the characteristics of the membrane (pore size), size and charge of the retained particles or molecules, and pressure exerted on the membrane [31, 32]. In membrane filtration the driving force for the separation is a pressure gradient which is imposed through the semi-permeable membrane. Suspended solids or solutes are retained in the so-called retentate, while water and non-retained solutes pass through the membrane in the permeate [31, 32].

Microfiltration (MF) membranes have the largest pores (0.1 μm to 10 μm) and the highest hydraulic permeability. These values corresponds to the typical size of suspended solids, colloids and bacteria; however, MF membranes can only be used as a disinfection barrier if actions are taken against bacterial regrowth [31-33].

Ultrafiltration (UF) membranes have smaller pores (2 to 100 nm) and the hydraulic permeability is considerably lower than in MF. A typical application for these membranes is to retain dissolved macromolecules like the largest molecules of the natural organic material [31, 32, 34].

Nanofiltration (NF) is a membrane filtration process used most often with low total dissolved solids in water such as surface water and fresh groundwater, with the purpose of softening (polyvalent cation removal) and removal of infection by product precursors such as natural organic matter and synthetic organic matter. In nanofiltration the pore sizes are smaller than

in UF, typically around 1 nm, this makes NF suitable for the removal of relatively small organics, *i.e.* organic micro pollutants and colour from surface water or groundwater and degradation products from effluent of biologically treated wastewater. Furthermore, NF membranes can also have a surface charge that allows the removal of ions with a size below the pore size of the membrane [31, 32, 35].

Reverse osmosis (RO) is a water purification technology that also uses homogeneous (*i.e.*, non-porous) semipermeable membranes. The applied pressure is used to overcome the osmotic pressure. Rejection is not just a result of filtering, but solution-diffusion mechanisms will determine the permeation of the dissolved species. The low hydraulic permeability of reverse osmosis membrane requires high pressures and, consequently, relatively high energy consumption. This effect is even more pronounced in the presence of an osmotic pressure due to high concentrations of dissolved components that counteract the effect of the exerted pressure [31, 32, 36].

The characteristics of all these processes and membranes are summarized in Table 1 and Figure 2 and 3.

Table 1 Overview of membrane processes and their characteristics ([31]).

	Microfiltration	**Ultrafiltration**	**Nanofiltration**	**Reverse Osmosis**
Hydraulic Permeability ($L/h.m^2.bar$)	> 1000	10 – 1000	1.5 - 30	0.05 – 1.5
Pressure (bar)	0.1 - 2	0.1 – 5	3 - 20	5 – 120
Pore size (nm)	100 - 10000	2 – 100	0.5 - 2	< 0.5
Rejection	Particles	Multivalent ions, macromolecules, particles	Multivalent ions, Small organic compounds, Macromolecules, particles	Monovalent ions, multivalent ions, Small organic compounds, Macromolecules, particles
Separation mechanism	Filtration	Filtration	Filtration, charge effects	Solution-diffusion
Applications	Clarification, pre-treatment, removal of bacteria	Removal of macromolecules, bacteria, viruses	Removal of multivalent ions, relatively small organics	Ultrapure water, desalination

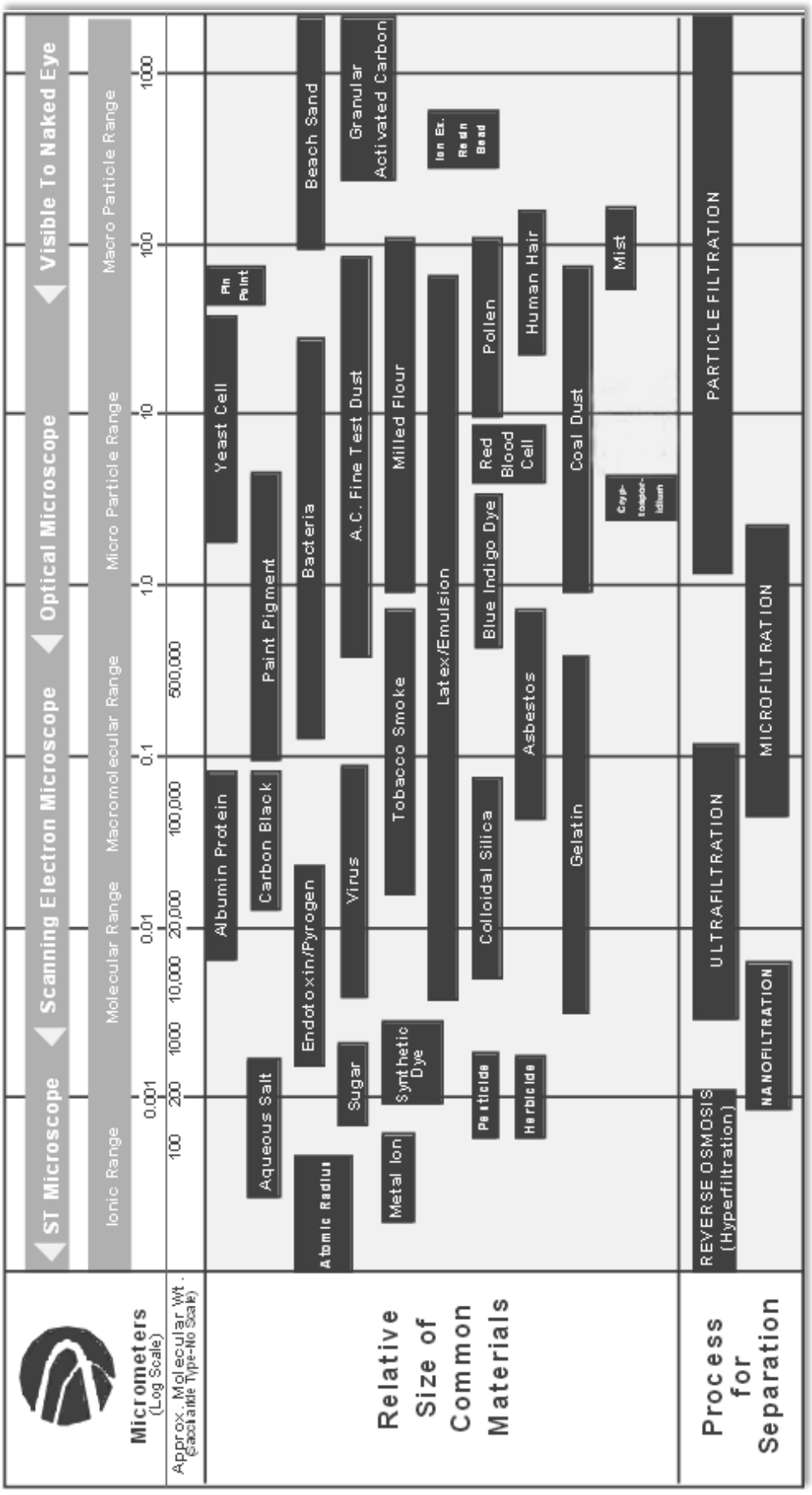

Figure 2 Pressure-driven membrane process spectrum (adapted from [37]).

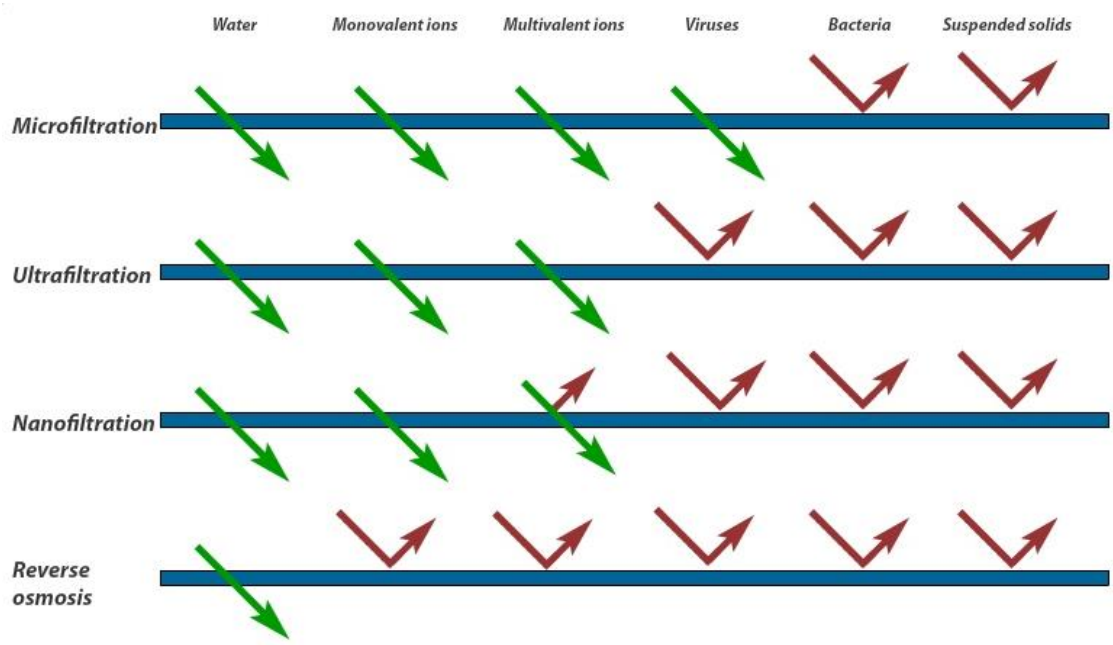

Figure 3 Membrane process characteristics: microfiltration, ultrafiltration, nanofiltration and RO distinguished (adapted from [38]).

1.2.2 Membranes applications

Membrane technology can be used in a large number of applications such as solid-liquid separation, concentration, buffer exchange, purification and sterilization [25, 27, 39]. Membrane technology not only has been extensively used for several applications in downstream processes, but in upstream processes too, which leads to a demanding role in the purification of biotechnology products [19, 29]. Furthermore, membrane processes are also used for water purification [27, 37], nucleic acids (pDNA and RNA) recovery and purification [15, 20] and gas–liquid contacting and emulsification [24]. In Table 2 are presented some commercial available membranes, as well as their composition and applications.

Table 2 Applications of the commercially available membranes used in membrane processes ([29, 32, 37, 39]).

	Commercially available membranes	**Materials used to produce membranes**	**Applications**
MF	*Nylaflo* (Pall Corporation) *GVWP* (Millipore) *MCE* (Advantec Toyo Corp.)	Cellulose acetate Poly(vinylidene fluoride) Polyamides Polyolefins Nylon Poly(tetrafluoroethylene)	Drinking water treatment Clarification Sterile filtration
UF	*FSM0.45PP* (Alfa Laval) *3038*, *3065* and *3028* (IRIS) *ES625* (PCI Membrane Systems)	Polyacrylonitrile copolymers Aromatic polyamides Polysulfone Poly(vinylidene fluoride)	Concentration Buffer exchange Desalination Sterile Filtration Biomolecule recuperation Clarification
NF	*MPS-44* (Koch Membrane) *NTR7250* (Nitto-Denko) *NF55* (Dow)	Aromatic polyamides Cellulose acetate	Desalination Salt separation Waste water treatment
RO	*ES20* (Nitto-Denko) *UTC-70* (Toray) *NCM1* (Hydranautics)	Cellulose acetate Polyamide	Ultrapure water production Desalination Waste water treatment

1.2.3 Membrane properties

A membrane is a semi-permeable barrier that is used to control transport of some kind of species. When the transport direction is out of a system it is called separation; when it is into the system it is called membrane contacting. The cause of transport through a membrane is a difference in chemical potential between both sides. This difference may be due to a gradient in temperature, pressure, concentration or electrical potential [24]. The mechanisms for transport strongly depend on membrane morphology. Two typical morphologies can be distinguished: porous and dense (homogeneous). Dense membranes are permeable for single molecules and have two major characteristics: transport by solution-diffusion model and intrinsic selectivity. Solution-diffusion transport is the concentration gradient diffusivity, *i.e.*, transport occurs only by diffusion, and can explain dialysis, reverse osmosis, gas permeation and pervaporation, and it is clearly material dependent. The component that needs to be transported must first be dissolved in the membrane. In solution-diffusion model it is assumed that the chemical potential of the feed and permeate fluids are in equilibrium with the adjacent membrane surfaces such that appropriate expressions for the chemical potential in the fluid and membrane phases can be equated at the solution-membrane interface [24, 40]. Intrinsic selectivity is the indication of the membrane separation efficiency and in combination with the hydraulic permeability it indicates the general performance of the membrane [24].

In porous membranes the transport mechanism is completely different. Transport occurs through the empty spaces (pores) of the membrane. However, the interaction with the internal membrane surface can play a crucial role. In respect to membrane morphology the surface and volume porosity, pore size distribution and tortuosity are important parameters for its performance. Tortuosity is a factor used to correct the deviation of pore shape from perfect cylinders. It is defined by the ratio of the average path length through the pores and the membrane thickness. The pore sizes range goes from micrometers to below 1 nm and the porosities range goes from more than 80% for micrometer-sized pores to less than 2% for nanometer-sized pores. An important property of membranes used in pressure-driven techniques is the hydraulic permeability, L_p, which is the ratio of the observed permeate flux to the imposed pressure. Both the porosity, the pore size and the membrane tortuosity affect the value of the observed L_p. L_p is also dependent on the viscosity of the permeate and therefore is temperature dependent. In respect to ultrafiltration membranes, another important property is the molecular weight cut-off, which indicates the molecular weight of the macromolecules 90% retained by the membrane; this gives an approximate indication of the pore size. In respect to the retentive properties of membranes it is also important to define the concepts of sieving coefficient and rejection. The sieving coefficient of a certain solute or particle relates the concentration of component in permeate to that in the feed. The rejection is defined as one minus the sieving coefficient [24].

Membranes can be operated in two modes (Figure 4): “dead-end” mode and “cross-flow” mode. In the dead-end mode a solution contained in a reservoir is transported towards the membrane.

The components rejected by the membrane will accumulate at the membrane surface and eventually will diffuse back to the bulk of the solution in the reservoir. On the other hand, in cross-flow mode, the feed flows parallel to the membrane surface. In both cases the stream that passes through membrane is called "permeate", while the remainder is defined as "retentate". Therefore, in a cross-flow system the permeate stream flows perpendicular to the feed stream but in a dead-end system the permeate flows in the direction of the feed [24].

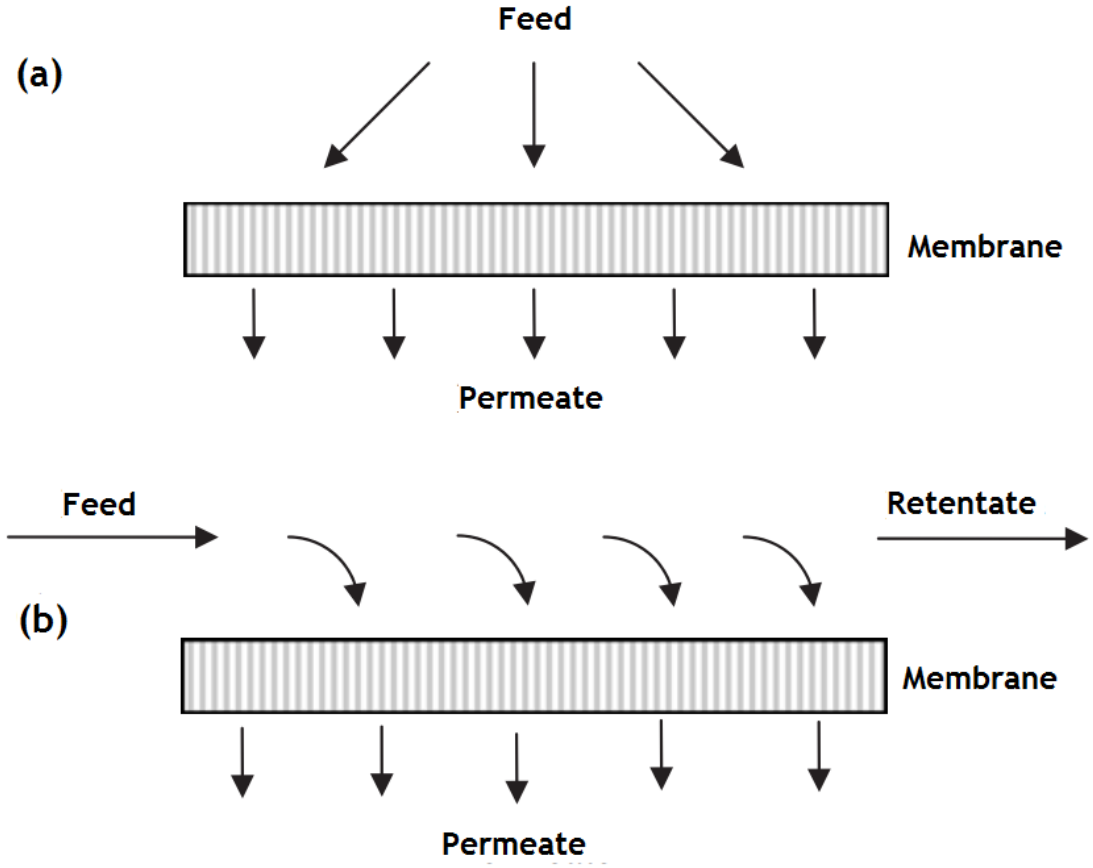

Figure 4 Comparison between a (a) dead-ended filtration and a (b) cross-flow filtration (adapted from [29]).

1.2.4 Factors that affect the filtration process

In the filtration process, there are certain factors that affect the filtration, these factors are, mainly membrane selectivity, the flux and the system capacity [27].

The selectivity of the membrane is determined by the pore size distribution and the membrane surface properties, *i.e.*, highly selective ultrafiltration membranes can be developed using electrically charged membranes that have very high retention of macromolecules with the same polarity and similarly. By turn, adsorptive membranes can provide highly selective separations based on the specific binding of several components on the surface of the membrane [41, 42]. The selectivity is directly related to the solute filtering coefficient:

$$S = \frac{C_f}{C_F} \qquad (1)$$

where C_f is permeate solution and C_F is the feed solution [27].

The flux is evaluated using the actual feedstock of interest, being typically less than the value predicted from the clean membrane permeability, due to fouling and concentration polarization effects [43]. The pure water flux is related to the membrane hydraulic permeability:

$$L_p = \frac{J_v}{\Delta P} \qquad (2)$$

where J_v is the flux (volumetric flow rate per unit membrane area) and ΔP is the transmembrane pressure difference [27]. The membrane fouling can arise from adsorption on and within the membrane pores and/or from the formation of a deposit on the external surface of the membrane (Figure 5). Concentration polarization refers to the accumulation of completely or partially retained solutes at the upstream surface of the membrane due to bulk mass transfer limitations of the membrane. The dominant effect in protein ultrafiltration is the reduction in the effective pressure driving force due to osmotic pressure effects [27]. The extent of the concentration polarization can be controlled by adjusting the fluid flow characteristics, typically by providing high local shear rates in cross-flow filtration modules or by stirring the feed in "dead-end" filtration [44, 45].

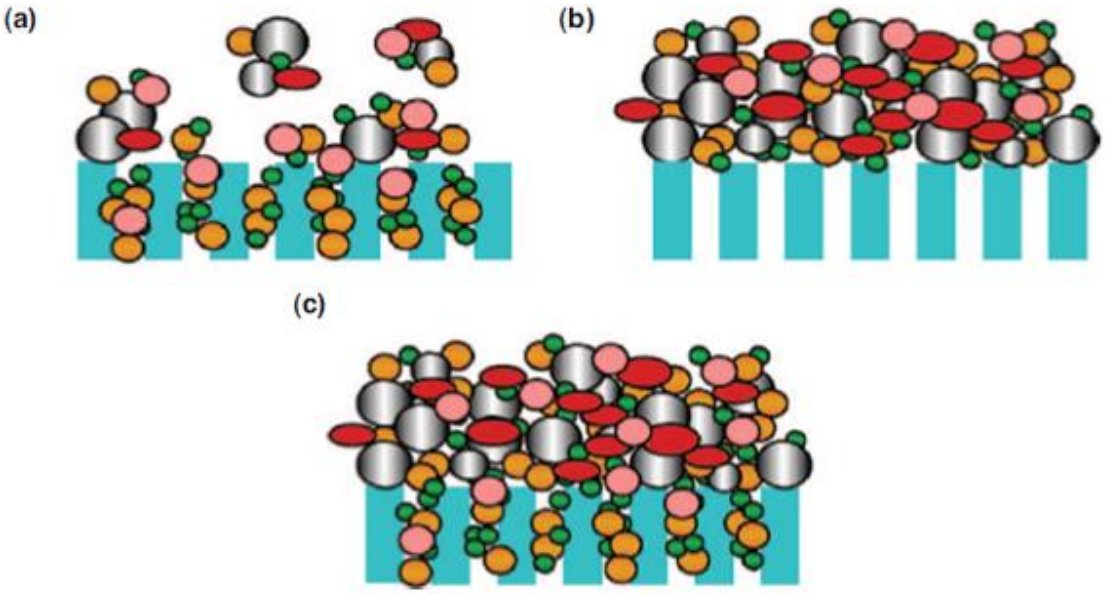

Figure 5 Membrane fouling can occur due to adsorption within the membrane pores (a), adsorption on the membrane surface (b) or by both of them (c) (adapted from [46]).

The system capacity is defined as the volume of feed that can be processed per unit membrane area, before the membrane needs to be regenerated or replaced. For membrane processes

operated at a constant transmembrane pressure, the capacity is typically defined as the point at which the filtrate flow rate has dropped to less than 10% of its initial value or below a pre-determined flux that is required for a particular application. For operation at constant filtrate flux, the capacity is defined by the maximum pressure drop that can be tolerated by the system, and can be limited by the membrane. The adsorptive membrane capacity is defined by the appearance of an unacceptable level of a key component in the flow-through stream (referred to as breakthrough). Breakthrough is determined by both the equilibrium (static) binding properties of the membrane in combination with any mass transfer limitations in the device. The capacity of depth filters can be determined by either the breakthrough of a key component or by an unacceptable pressure drop [27].

1.3 Nanofibrous membranes

Electrospinning is an easy and cheap method of producing nanofibres [21]. The simplicity of this procedure and the wide range of applications found in recent years, including tissue engineering applications, such as bone repair, wound healing and drug delivery [47-49], sensors and biosensors production [50], polymeric conductive membranes[1] development [51] and filtration[2] [52-54]. Such variety of applications leads to an increased interest in developing new types of electrospun nanofibre membranes [55].

The electrospinning apparatus consists in three basic components (Figure 6): a needle attached to a syringe filled with a polymer solution; a grounded collector plate; a high voltage power supply, connected between the capillary and the collector; and a syringe pump that is usually used to control the feeding rate of the polymer solution. A charged polymer solution flowing out of the needle is accelerated towards the grounded collector through the application of a strong electrostatic field [55, 56]. This electromagnetic field causes the droplet to emerge from the needle to undergo deformation into a conical shape, known as the "Taylor cone" (Figure 7) [57]. When a critical value is attained (the repulsive electrostatic force overcomes the surface tension) a fine jet of the solution emerges from the "Taylor cone". The jet undergoes twisting instability and a characteristic whipping motion due to the charge-charge repulsion that occurs between the excess charges presented in the jet (Figure 6). During this phase, the jet is drawn by at least two orders of magnitude, the solvent evaporates and the dry fibres deposit onto the collector [56, 58-60]. A polymer melt, instead of a polymer-solvent solution, can also be used by a heating system that surrounds the reservoir and maintains the temperature [56, 61].

[1] Applied as electrostatic dissipation, corrosion protection, electromagnetic interference shielding, photovoltaic device, fabrication of tiny electronic devices.
[2] Used in air filtration applications for more than a decade, and currently in solid-liquid filtration.

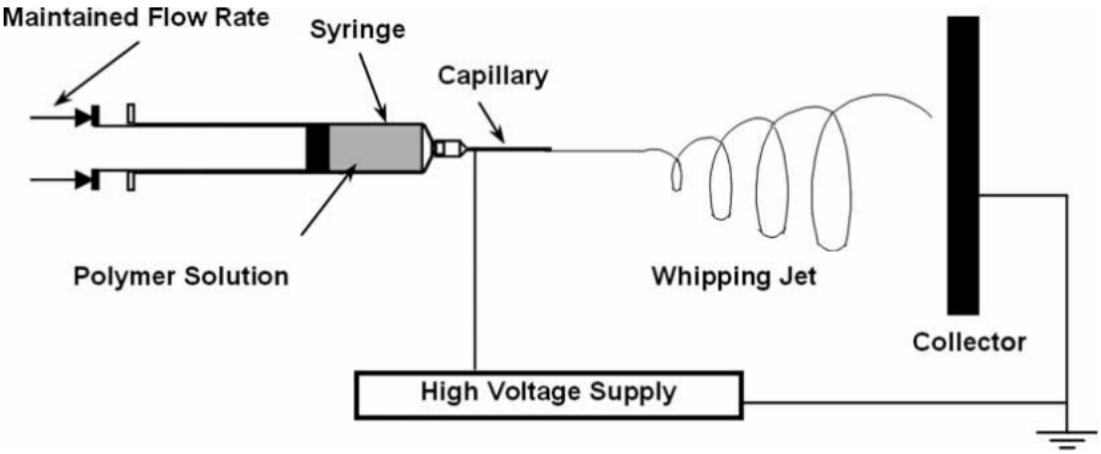

Figure 6 Representation of the electrospinning apparatus (adapted from [56]).

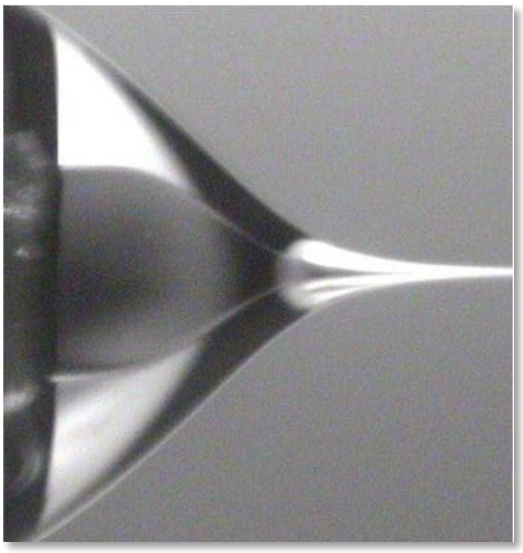

Figure 7 Image representing the Taylor cone (adapted from [56]).

1.3.1 Parameters that influence the production of nanofibrous

The fibre structure is affected by different factors such as the density of chain entanglements, solution conductivity, solution viscosity, strength of applied field, polymer feed rate, needle size and diameter, and the distance between the needle and the collector. Moreover, the surrounding conditions such as temperature, humidity and air velocity also affect the morphology of the fibres.

The density of chain entanglements, as shown in Figure 8, is an important parameter since it prevents the occurrence of the phenomena known as Rayleigh instability, and is related to the solution viscosity (directly controlled by the molecular weight of the polymer and the solution concentration). The chain entanglements prevent the jet to break up and, therefore, the

Rayleigh instability[3] [62] does not occur, which result into a continuous fibre formation. If the density of chain entanglements in a given solution is less than a critical value, the jet breaks up due to insufficient resistance to the electrostatic field [63-65]. If the entanglements in the chains are present but the amount of the chain superposition is below the critical value, then Rayleigh instability is not completely eliminated, leading to the formation of fibres with beaded morphologies [64, 65].

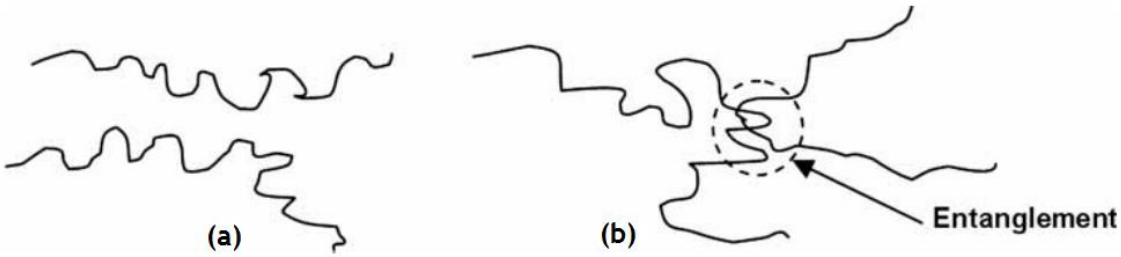

Figure 8 Illustration of polymer chain entanglement: (a) isolated polymer chains, (b) entangled polymer chains (adapted from [56]).

An increase in the solution viscosity, beyond necessary minimum, increases the visco-elastic force which opposes coulombic force and therefore leads to an increase in fibre size. An increase in the strength of the field and/or conductivity of the polymer solution could be expected to lead to a decrease in fibre size [55, 56].

Other parameter that affects electrospinning process and fibre morphology is the solution conductivity. Fluids with high conductivity have high surface charge density, and under the influence of an electric field, suffer an elongation force on the jet, which is caused by the self-repulsion of the excess charges at their surface. This inhibits the Rayleigh instability, enhances whipping, and leads to the formation of thin fibres [63, 66, 67].

A higher feeding rate of the polymer solution and/or larger size of the needle diameter increases the fibre size, and a larger distance between needle tip and collector plate decreases fibre size. These effects are not linear and do not necessarily mean that the quality of the product is maintained but they give a general idea about the trends [55]. For each polymer type and solvent system, there is usually a relatively narrow set of manufacturing conditions that provide optimal results [55, 56].

At last another parameter affecting the fibre morphology is the interactions between the polymer and the solvent, where the molecular weight of the polymer does affect the process. If certain physical properties are required for the polymer solution, it is very important to select

[3]Explains why and how a falling stream of fluid breaks up into smaller packets with the same volume but less surface area.

the right solvent or combination of the appropriate solvents, since the first and key step in the electrospinning process is the polymer dissolution in a suitable solvent [55]. The dielectric constant (table 3) and the boiling temperature of the solvent are absolutely decisive when selecting the correct one to produce nanofibrous. Solvents with a low dielectric constant will improve the dissolution of the polymer charged chains by dispersing the ion pairs, enhancing the conductivity and, therefore, reducing the need of applying extreme voltages [56]. Furthermore, solvents with low boiling point will evaporate faster from the polymer surface, upon fibre formation [55, 56].

Table 3 Properties of different solvents used in electrospinning process ([55]).

Solvent	**Surface tension (nM/m)**	**Dielectric constant**	**Boiling point (°C)**
Chloroform	26.5	4.8	61.6
Dimethyl formamide	37.1	38.3	153
Hexafluoro isopropanol	16.1	16.70	58.2
Tetrahydrofuran	26.4	7.5	66
Trifluoro ethanol	21.1	27	78
Acetone	25.20	21	56.1
Water	72.8	80	100
Methanol	22.3	33	64.5
Acetic acid	26.9	6.2	118.1
Formic acid	37	58	100
Dichloro methane	27.2	9.1	40
Ethanol	21.9	24	78.3
Trifluoro acetic acid	13.5	8.4	72.4

1.3.2 Polymeric Nanofibrous

The ability of reducing the diameter of polymeric fibre materials from micrometers to nanometers enables several remarkable features, such as very large surface area to volume ratio, versatility of the nanofibrous surface functionalization and superior mechanical performance (e.g. stiffness and tensile strength) that allow the production of fibres with a wide variety of sizes and shapes [68].

The morphological, chemical and mechanical characterization of the nanofibrous is usually performed. The fibre diameter, distribution, orientation and morphology (*i.e.* cross-section shape and surface roughness) are usually characterized by scanning electron microscopy, field emission scanning electron microscopy, transmission electron microscopy and atomic force microscopy [55, 69-74]. The characterization of the molecular structure (chemical characterization) of a nanofibre can be performed by Fourier transform infrared spectroscopy and nuclear magnetic resonance techniques. If two polymers are blended together for the fabrication of nanofibrous, not only the structure of the two materials can be detected but the intermolecular interaction can be determined by the use of these methods; the characteristic peaks from each component of the membrane must be found in the spectra of the final product [55, 75]. The mechanical characterization, which consists in the precise measurement of mechanical properties of the nanofibrous matrix, is crucial especially for biomedical applications. For example, for nanofibrous acting as scaffolds, they must be able to withstand the forces exerted by the growing tissue or during physiological activities and related biomechanics and therefore, their mechanical characterization should be performed. The mechanical characterization is achieved by applying tensile test loads to specimens prepared from the electrospun ultrafine non-woven fibre mats. The tensile tests consist in stretching the membrane to the point of rupture and analyse its resistance. During the mechanical characterization of single nanofibrous, sufficient care must be taken in sample mounting in order to avoid severe damage or sample manipulation [55, 76, 77].

Electrospun fibres can be applied in different areas, such as filtration, wound healing, affinity membrane, protective clothing, energy generation, enzyme immobilization, drug delivery, tissue engineering and biosensors (Figure 9) [78, 79]. For filtration, the channels and structural elements of a filter must be matched to the scale of the particles or droplets that will be captured in the filter. Thus, we can take advantage of the unique properties of electrospun membranes consisting of very-small-diameter fibres [55].

In wound healing, an ideal dressing should have certain characteristics such as haemostatic ability, efficiency as bacterial barrier, absorption aptitude of excess exudates (wound fluid/pus), appropriate water vapour transmission rate, adequate gaseous exchange capability, capacity to conform to the contour of the wound area, functional adhesion (*i.e.*, adherent to healthy tissue but non-adherent to wound tissue) painless to patient and ease of removal, and finally have a low cost [55, 80].

Affinity membranes are a broad class of membranes that selectively capture specific target molecules (or ligands) by immobilizing a specific ligand onto the membrane surface. They reflect technological advances in both fixed-bed liquid chromatography and membrane filtration, and combine both the outstanding selectivity of the chromatography resins and the reduced pressure associated to filtration membranes [55, 81, 82].

Electrospun nanofibre membranes have been recognized as potential candidates for protective clothing applications, because of their low weight, large surface area, high porosity (breathable nature), great filtration efficiency, resistance to penetration of harmful chemical agents in aerosol form and their ability to neutralize the chemical agents without impedance of the air and water vapour permeability to the clothing. Protective clothing should have some essential properties, ensured by the nanofibrous, such as low weight, breathable fabric, air and water vapour permeability, insolubility in all solvents and enhanced toxic chemical resistance [55, 83, 84].

Polymeric conductive membranes also have the potential to be applied for electrostatic dissipation, corrosion protection, electromagnetic interference shielding, photovoltaic devices and fabrication of tiny electronic devices or machines such as Schottky junctions, sensors and actuators etc., as the rate of electrochemical reactions is proportional to the surface area of the electrode [55, 85, 86].

Immobilization of enzymes on inert insoluble materials is an active area of research for improving the functionality and performance of enzymes for bioprocessing applications since the immobilized enzymes offer several advantages such as reusability, better control reaction and are more stable than soluble ones. The performance of immobilized enzymes depends greatly on the characteristics and structure of the carrier materials and the modification of the carriers, such as rendering biocompatibility, hydrophilicity, etc. [87]. The fine porous structure of electrospun fibres membranes can effectively relieve the diffusion resistance of the substrates/products and can greatly increase the catalysing ability of the immobilized enzymes due to the large specific surface area [55, 88, 89].

Controlled drug release at a defined rate over a definite period of time is possible with biocompatible delivery matrices of polymers, biodegradable polymers are therefore mostly used as drug delivery systems to deliver therapeutic agents because they can be easily designed for programmed dissemination in a controlled fashion [55, 90]. Nanofibre mats have been applied as drug carriers in drug delivery systems because of their high functional characteristics and because drug delivery system that rely on the principle that the dissolution rate of a particulate drug increases with the increase of the surface of the drug. Also, the large surface area associated with nanospun fabrics allows fast and efficient solvent evaporation, that provides the incorporated drug limited time to recrystallize which favours the formation of amorphous dispersions or solid solutions [55, 91].

For engineered living tissues, a biodegradable scaffold is generally considered as an indispensable element. Nanofibres are used as temporary templates for cell adhesion, proliferation and differentiation in order to repair and restore the damaged tissue, *i.e.*, to reproduce the native extracellular matrix (ECM) environment. There has been an increased rush in the use of electrospinning techniques to create nanofibrous scaffolds for tissue engineering due to the reports that indicate that these scaffolds positively promote cell–matrix and cell–cell interactions with the cells having a normal phenotypic shape and gene expression [55, 92].

Finally, biosensors, which typically consist of a bio-functional membrane and a transducer, have been widely used for environmental, food, and clinical purposes. There are many parameters that affect the performance of a sensor which includes sensitivity, selectivity, response time, reproducibility and aging, all of which are dependent directly on the property of the sensing membrane used. Since there is a strong need for detection of gases and biological substances when they are present in low concentrations, sensitivity plays a very critical role. Modern biomedical sensors with advanced micro fabrication and signal-processing techniques are becoming more and more accurate and inexpensive nowadays [55, 93]. Electrospun nanofibrous membranes have received great attention for applications as sensors because of their unique large surface area which is the most desirable property for improving the sensitivity of conductimetric sensors, a larger surface area will absorb more gas analyte and change the sensor's conductivity more significantly. Silk fibroin membranes-based biosensors have been extensively used for analysing various substances such as glucose, hydrogen peroxide and uric acid [55, 94, 95].

In this work, a poly ε-caprolactone support was prepared by a conventional electrospinning process. This polymer was selected based on the good mechanical properties that PCL meshes present [21, 96] and also for being environmentally friendly [21, 97]. A coating based on an electrospun mixture of two polymers, *k*-carrageenan and polyethylene oxide (PEO), was deposited on the PCL support. *k*-carrageenan was selected for Electrospun Nanofibre Membranes (ENMs) coating due to its high hydrophilicity, relatively low cost, the ability of producing small diameter fibres by electrospinning, when mixed with PEO, and due to their sulphate groups [21, 98, 99]. This asymmetric arrangement of two different layers provides the membrane with suitable mechanical robustness whereas separation selectiveness is regulated predominantly by the ultrathin layer of nanofibres [21].

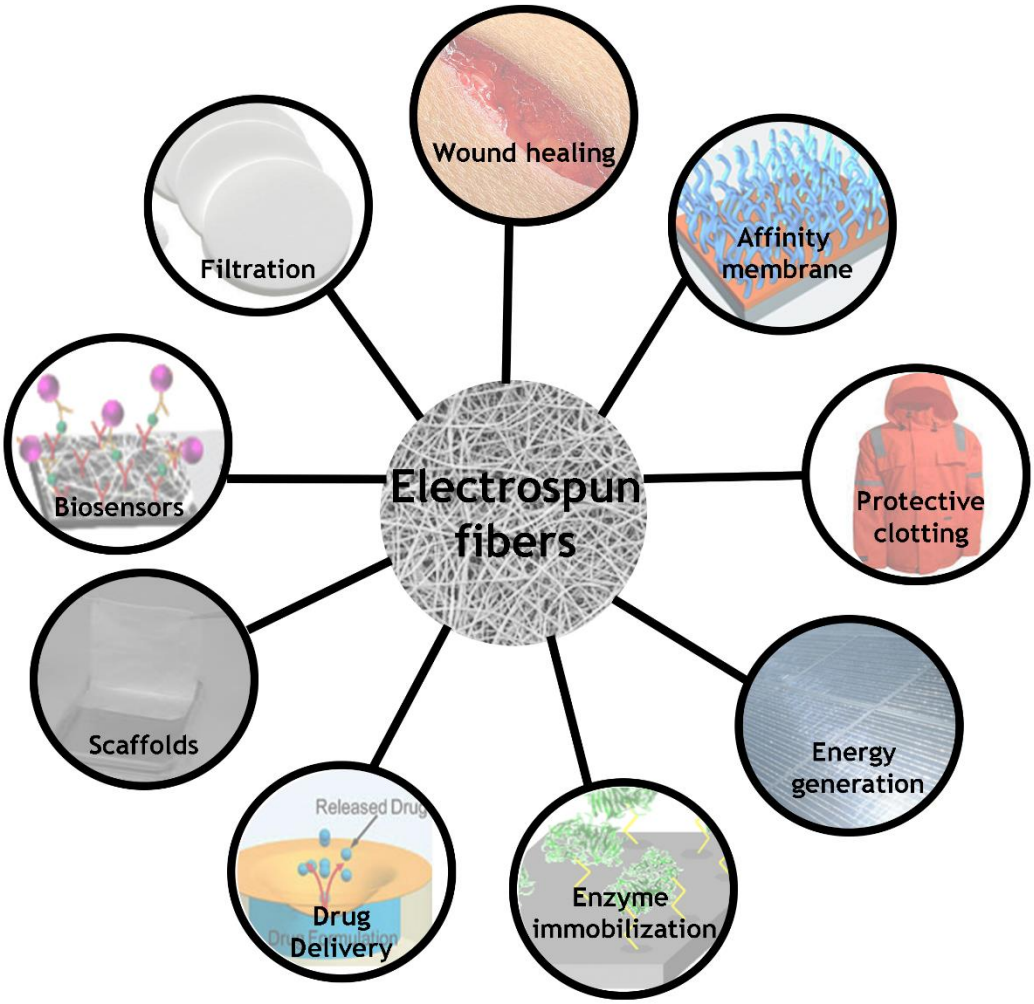

Figure 9 Scheme of the applications of electrospun nanofibres in different sectors.

1.3.3 Application of nanofibrous membranes on separation processes

Electrospun nanofibrous membrane have successfully been developed and used for the production of high-performance air filters. The filtration efficiency, which is closely associated with fibre thickness, is one of the most important concerns for filter performance. Generally, when filter efficiency increases linearly with the decrease of the thickness of the membrane filter and the applied pressure increases. The enhanced filtration efficiency at the same pressure drop is possible with fibres having diameters less than 0.5 μm [55, 100]. Electrospun membranes offer a wide set of advantages for filtration applications, such as higher porosity (typically around 80%), higher surface area to volume ratio and high surface cohesion (which facilitates particle entrapment and, therefore, improves the filtration efficiency), lower base weight, and continuously interconnected pores, when compared to conventional polymer and ceramic membranes. These attributes can directly improve the flux performance without sacrificing the contaminant rejection ratio [101, 102]. The consistent production of very small diameter fibres enables the removal of unwanted particles at the submicron scale, which is clearly an advantage of the electrospinning membranes [55].

Electrospinning membranes have been reported for application in separation processes, especially in pressure-driven separations, such as microfiltration, ultrafiltration or nanofiltration [103-105], but for this type of application it is required a support that provides mechanical strength, unlike conventional cast membranes. Consequently, nowadays, electrospinning membranes used in filtration technology are based in hybrid systems, *i.e.*, electrospun nanofibres are placed over a support and combined in various layers or blended together with micron scale fibres [106].

1.4 Hydrogel membranes

Currently, there are several UF membranes commercially available that can be used for pDNA purification [20, 23]. Considering the size of pDNA molecules, surface modification of microfiltration membranes also arises as a possible choice, offering the possibility of adjusting the desired selectivity in each particular case. Several studies have shown the enhancement of membrane properties such as resistance to fouling by proteins, biocompatibility, introduction of electric charge and improved hydrophobicity through surface modification methods [107-109]. In this work, a hydrogel coating (agarose) was impregnated to a commercial MF membrane with 0.22 μm of nominal pore diameter (membrane selected based on its cost-effective value, mechanical strength and heat resistance which facilitates the impregnation of a hot solution [110]) by an adaptation of a method described in literature [111]. The deposition of the agarose layer and its impregnation through the porous structure of the MF membrane was expected to provide a substantial increase of pDNA rejection comparing to the non-modified membrane. From the best of our knowledge, it is the first time that a modified MF membrane is evaluated for its possible application in a pDNA purification process.

1.4.1 Hydrogel characteristics

The widespread use of hydrogels in areas such as liquid chromatography, drug delivery, and therapeutic implants, and the existence of various body tissues with gel-like characteristics (*i.e.* connective tissue and basement membranes) make it important to understand the rates of plasmids transmissions and other macromolecules through these materials [111]. In separation and purification of biological macromolecules, it is important to study the gel filtration medium. The gels based on cross-linked polysaccharides have been regarded as close to ideal and most media on the market today are based on these materials. However, even if hydrophilicity and inertness are necessary properties of a functional gel filtration medium, there are a number of other requirements, such as adequate pore size distribution, rigidity, physical and chemical stability, which also have to be fulfilled. Media-based on cross-linked agarose share most of these properties [112].

In the present work, agarose was chosen also for its hydrophilic and thermo-responsive character; this linear polysaccharide extracted from marine algae, consisting of 1,4-linked 3,6-anhydro-α-l-galactose and 1,3-linked ß-d-galactose derivatives forms a thermo-reversible gels, when a homogeneous solution is cooled from 90 ºC to a temperature below the ordering temperature, which is around 35 ºC. This phenomenon is based on the physical cross-linking of the helical structure formed by the agarose polymer. The physical cross-linking gives rise to a three dimensional network of aggregated polymer molecules; its pore-size distribution only depends on the agarose concentration of the starting solution. By covalent cross-linking the aggregated polymers in an aqueous environment, the chemical and physical stability of agarose gels can be considerably improved [112]. Agarose gels have been investigated in several applications due to their suitable properties for membrane modification and impregnation, and the mechanical properties presented can be easily tailored by varying the polymer concentration [113, 114]. Due to its physical properties, when agarose is solubilized in water, it forms a gel with a rigid network, resulting on a three-dimensional porous structure providing a rigid assembly when lies at room temperature (RT) [114]. Agarose gel appears as an apyrogenic, colourless and transparent gel, which is viscous-elastic at temperatures above 45 ºC [115].

1.5 Objectives

In this work, electrospinning and impregnation techniques were used in order to produce filtration membranes to be applied in plasmid DNA purification. The present master thesis work plan had the following aims:

- Produce electrospun membranes using Poly *ε*-Caprolactone and Polyethylene Oxide/*k*-carrageenan, and modify a commercial microfiltration membrane by impregnation with a hydrogel (agarose);
- Characterization of the properties of the produced ENMs and modified MF membrane by Scanning Electron Microscopy, Attenuated Total Reflectance-Fourier Transform Infrared Spectroscopy, Energy Dispersive Spectroscopy, determination of the Contact Angle, Membrane Porosity and average pore size determination with reference solutes.
- Evaluation of performance of both membranes in pDNA purification.

Chapter II

Materials & Methods

2. Materials and methods

2.1 Materials

Acetone (MW = 58.08 g/mol) was purchased from Labsolve (Porto Salvo, Portugal) and agarose (MW = 120 kDa) was from Grisp (Porto, Portugal). Calcium chloride (MW = 110.99 g/mol), kanamycin sulphate, PEO (MW=300,000 g/mol), PCL (MW=80,000 g/mol) and Terrific Broth medium for bacterial culture were bought from Sigma-Aldrich (Sintra, Portugal). *k*-carrageenan (MW = 401.3193 g/mol) was obtained for FMC BioPolymer (Philadelphia, PA, United States). NZYMaxiprep kit for bacterial cell lyses and pDNA purification was acquired from NZYTech (Lisboa, Portugal) and Tris-HCl 10 mM was from IZASA (Lisboa, Portugal). A microfiltration *Nylaflo* membrane (pore diameter of 0.22 μm) was purchased from Pall Corporation.

2.2 Methods

2.2.1 Bacterial growth, cell lysis and pDNA purification

The plasmid production procedure was adapted from the literature [20, 21, 116]. The 6050 bp plasmid *pVAX1-LacZ* was amplified in a cell culture of *E. coli* DH5α. The fermentation was carried out at 37 ºC in 250 mL of Terrific Broth medium, supplemented with 50 μg/mL of kanamycin. Growth was suspended at the late log phase (OD_{600nm} ≈ 10-11) and the cells were harvested by centrifugation. Afterwards, pDNA extraction was performed using an NZYMaxiprep kit. That kit contains three buffers to perform the alkaline lysis, respectively:

- **Resuspension buffer (P1)**: solution of 50 mM Tris-HCl, pH = 8.00 and 10 mM EDTA;
- **Lysis buffer (P2)**: solution of 200 mM NaOH and 1% SDS (w/v);
- **Neutralization buffer (P3)**: Solution of 3 M of potassium acetate at pH = 5.00.

Besides the buffers, the kit also contains purification columns to obtain a pDNA free of contaminants. After the extraction and purification, pDNA was stored at 4 ºC before filtration assays.

2.2.2 Electrospinning setup

A conventional electrospinning system was used to produce the membranes. The apparatus was composed by a high power voltage supply (*Spellman CZE1000R, 0-30 kV*), a syringe pump (*KDS-100*), a plastic syringe with a stainless steel needle and an aluminium disk (radius 2.4 cm) connected to a copper collector. To produce fibres there must be a driving force generated by

the electromagnetic field created between the needle, which is positively charged by high voltage source, and the metal collector, which is grounded [21, 55].

2.2.3 Preparation of the polymer solutions

The PCL polymer solution (10% w/v) was prepared by dissolving the polymer in acetone, at 50 ºC, under constant stirring [117]. Meanwhile, a PEO/*k*-carrageenan solution was prepared by mixing and dissolving 6.75% (w/v) of PEO and 0.5% (w/v) of *k*-carrageenan in *MiliQ* water, under constant stirring too [118].

The solution of agarose (2% w/v) was prepared by dissolving the polymer in *MiliQ* water under constant stirring, at 90 ºC [119].

2.2.4 Electrospun nanofibre membranes production

To produce the support ENM, a PCL polymer solution (Figure 10a) was injected at a constant flow rate of 3 mL/h and subjected to an applied voltage of 15 kV and with the collector placed at 10 cm from the needle [117]. After the production of the support, the PEO/*k*-carrageenan polymer solution (Figure 10b and c, respectively) was deposited over the PCL ENM by electrospinning, in the same equipment, at a constant flow rate of 0.6 mL/h and an applied voltage of 18 kV, thereby obtaining a bi-layer membrane. At least, the Coated Electrospun Nanofibre Membrane (ENMC) was crosslinked in a calcium chloride solution for 24 h [21, 118]. From the obtained films, membrane disks were cut with suitable size to be used in the filtration cell, using a circular blade [21].

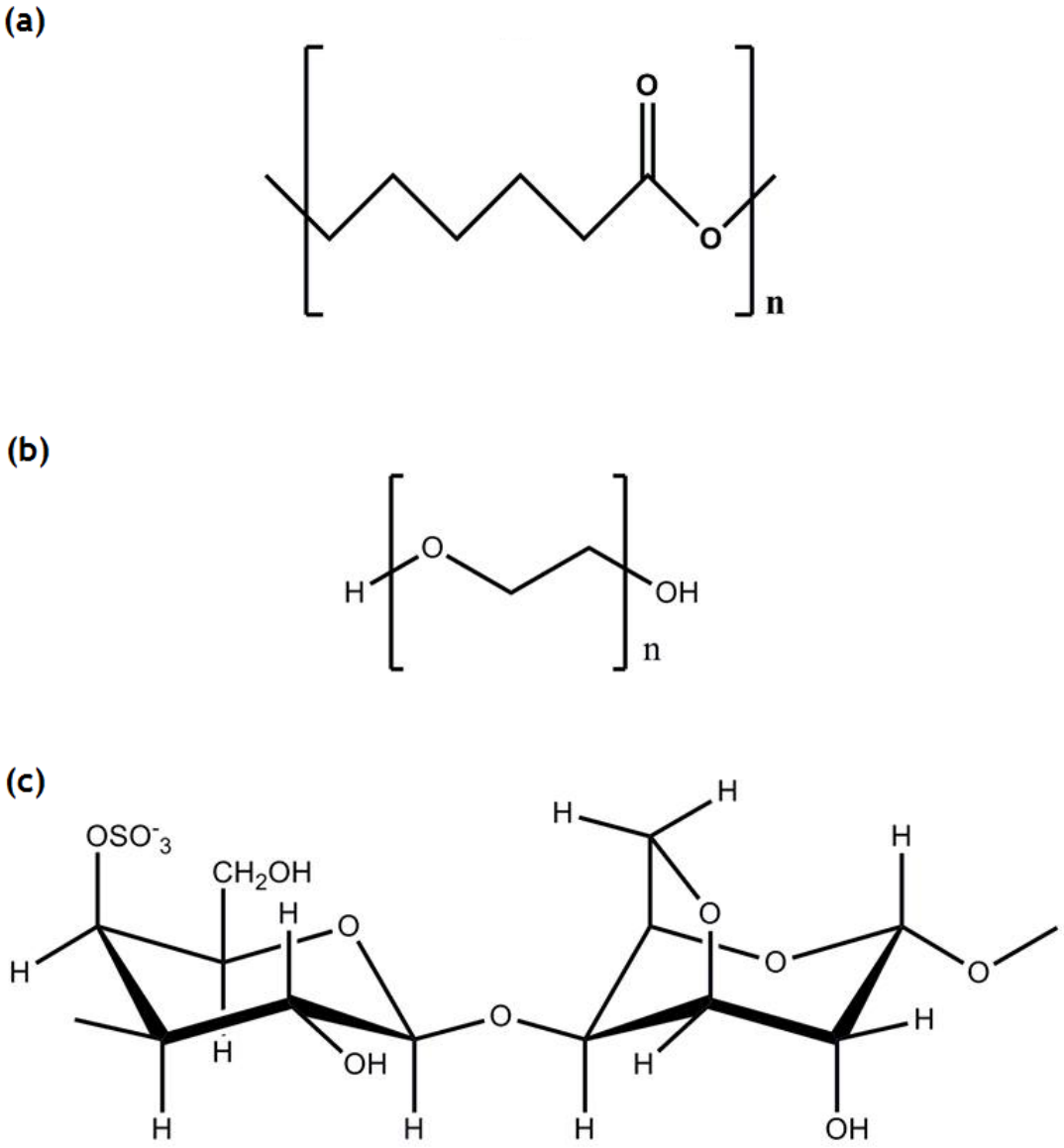

Figure 10 PCL (a), PEO (b) and *k*-carrageenan (c) chemical structure.

2.2.5 Modification of a commercial microfiltration membrane

A nylon 6,6 (Figure 11b) hydrophilic membrane, *Nylaflo* from *Millipore* was modified by agarose (Figure 11a) impregnation. The modification method was adapted from the literature [111] through the deposition of agarose to improve pDNA rejection (Figure 11a). An agarose solution (prepared by the method mentioned in section 2.2.3) was cooled down to a temperature of 70 °C and deposited over the MF membrane. To avoid air bubbles during the process, two glass plates were used and clamped. After 30 min., the membrane was cooled until reach the room temperature (RT) [119].

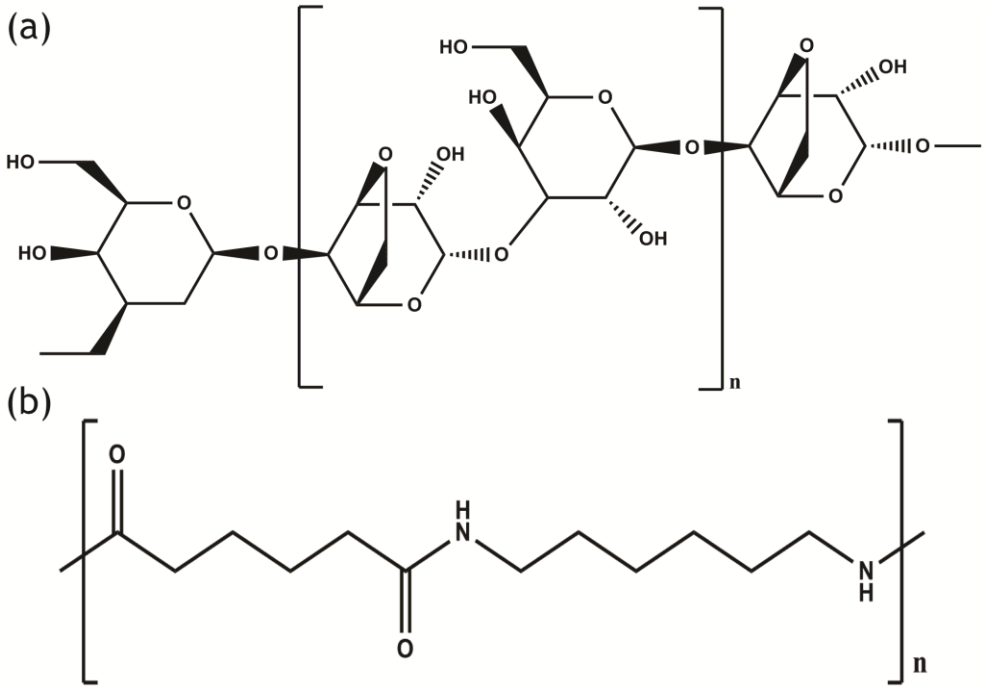

Figure 11 Agarose (a) and Nylon 6,6 (b) chemical structure.

2.2.6 Scanning electron microscopy

The morphology of all the membranes was analysed by SEM. Samples of ENMs were air-dried overnight and samples of modified-*Nylaflo* membrane were frozen using liquid nitrogen and freeze-dried overnight. Then, all the samples were mounted onto aluminium stubs with double adhesive tape and sputter-coated with gold using a Quorum Q150R ES sputter coater. The samples were analysed using a *Hitachi* S-3400N scanning electron microscope operated at an accelerating voltage of 20 kV and at different amplifications [21, 116].

The diameter distribution of the nanofibres in the ENMs was determined from 50 measurements, at least, using *ImageJ* (National Institutes of Health, Bethesda (MD), United States of America).

2.2.7 Attenuated total reflectance-fourier transform infrared spectroscopy

In infrared spectroscopy the radiation crosses the sample, being partially absorbed and partially transmitted. The resulting spectra represent the frequency of vibration between the atoms linkage from the sample, creating therefore, a specific spectra for those interactions [120]. PCL, *k*-carrageenan, PEO, polymer coated ENMs, agarose, *Nylaflo* and modified-*Nylaflo* spectra were acquired in the range of 4000 – 525 cm^{-1}, using a JASCO 4200 FTIR spectrophotometer, operating in ATR mode (MKII *GoldenGate*™ Single Reflexion ATR System). Data collection was performed with a 4 cm^{-1} spectral resolution and after 128 scans [21, 116].

2.2.8 Energy dispersive spectroscopy

In order to determine the percentage of the characteristic elements of the *Nylaflo* and modified-*Nylaflo* membranes, EDS (Bruker XFlash Detector 5010) analysis was carried out. For that, samples were placed on aluminium stub supports and air-dried at room temperature [121].

2.2.9 Contact angle determination

Contact angles of the membranes were determined using a *Data Physics* Contact Angle System OCAH 200 apparatus, operating in static mode. For each sample, solvent drops were placed at various locations of the analysed surface, at room temperature. The reported contact angles are the average of, at least, three measurements [21].

2.2.10 Membrane porosity determination

The membrane porosity method was previously described [21]. Briefly, the total porosity of the membranes was measured through the determination of the amount of ethanol absorbed by the membranes using the following equation [122]:

$$\mathrm{P}(\%) = \frac{W_2 - W_1}{d_{ethanol} V_{membrane}} \times 100 \qquad (3)$$

where W_1 and W_2 are the weight of the dry membrane and the weight of the wet membrane, respectively, $d_{ethanol}$ is the density of the ethanol at room temperature, and $V_{membrane}$ is the volume of the membrane. The latter was determined from the membrane area and by measuring the membrane thickness with a micrometer *Adamel Lhomargy* M120 acquired from *Testing Machines Inc.*, USA.

2.2.11 Plasmid DNA experiments

All the membrane filtration experiments were performed in a 10 mL stirred cell from Amicon/Millipore (Figure 12), model 8010, according to a procedure previously described in the literature [20, 123]. The filtration cell has a "dead-end" geometry. The membrane was positioned on a horizontal support which enables the permeate to be collected through a circular array of channels. Mass transfer of the retained compounds by the membrane, from the membrane surface back to the bulk of the solution, can be controlled by mechanical stirring of the solution. The filtration cell can be operated in two different ways: at constant pressure or constant flux (Figure 13).

At a constant pressure the liquid is forced to permeate through the membrane, but the flux is not easily controlled, only the transmembrane pressure. This method was used to wash the membrane, to determine hydraulic permeabilities of the membranes produced and to perform pDNA filtration tests with membranes with reduced hydraulic permeability.

When the constant flux method is used, a peristaltic pump is placed downstream of the membrane. With this method the flux can be directly controlled; this method is the ideal to be used for membrane characterization with reference solutes since solute rejections can be theoretically related with the permeate flux, the average pore size and the solute molecular size. However, this method can only be used when low transmembrane pressure gradients are generated.

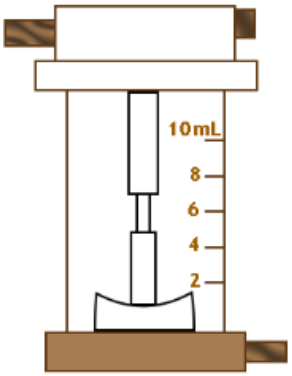

Figure 12 Scheme of the 10 mL stirred cell from Amicon/Millipore, model 8010.

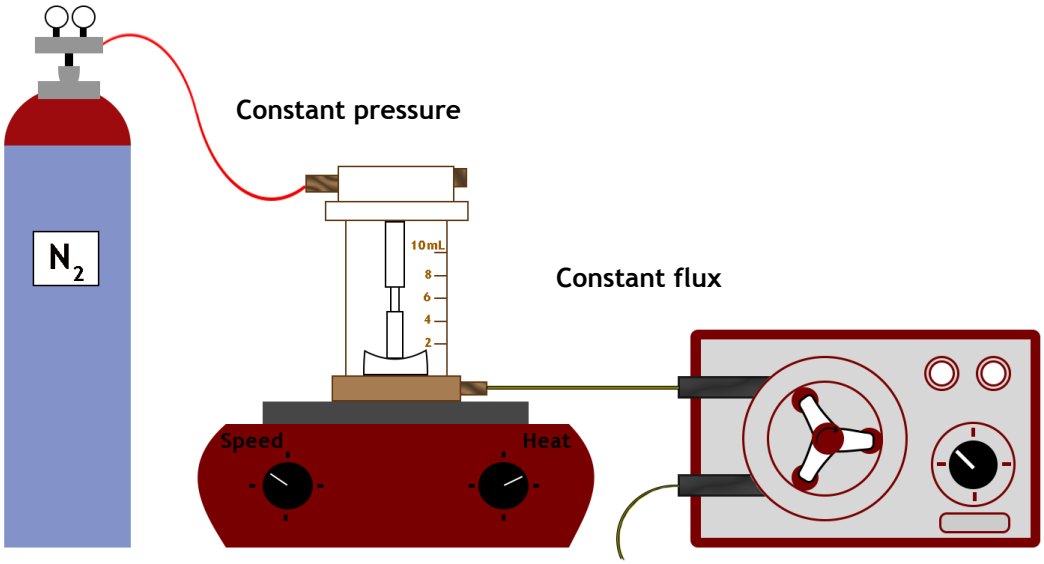

Figure 13 Scheme of the experimental set-up used for continuous filtration applying constant pressure and constant flux.

In each test, a new membrane disc was placed in the bottom of the filtration cell, being initially flushed with *MiliQ* water. Then, water was removed and 10 mL of 10 mM Tris-HCl 0.15 M NaCl (pH = 8.00) buffer were introduced in the filtration cell to determine the hydraulic permeability. This was obtained at different pressures with compressed nitrogen (ranging 0.025 bar to 0.1 bar) by measuring the flux over a period of time. Six permeability measurements were performed with each membrane, and the average value was considered as the hydraulic permeability of each membrane, L_p. To perform the filtration of pDNA solutions, the remaining buffer in the filtration cell was carefully removed and immediately after that, 5 mL of 10 mM Tris-HCl 0.15 M NaCl (pH = 8.00) buffer were placed in the cell with 100 µL of an aliquot of pDNA (recovered by the method mentioned in section 2.2.1). A continuous filtration of the content of the cell was performed by applying a constant pressure and four consecutive samples of 0.5 mL of permeate were collected; these four samples correspond to the total permeate collected in each run (the experimental setup is shown in Figure 13). The stirring speed was kept in all the experiments at 760 min^{-1} (previous calibration of the stirring system was performed).

2.2.12 Determination of Plasmid DNA concentration

Plasmid concentration was determined by Ultraviolet/Visible Spectroscopy at 260 nm. The absorbance of the initial pDNA solution (feed before the filtration assay) and the final concentrate (feed after the filtration assay) were determined in each run (as well as the absorbance of the four consecutive permeate collected samples previously mentioned). The 10 mM Tris-HCl, 0.15 M NaCl (pH = 8.00) buffer was used as the reference solution for measuring the absorbance due to pDNA.

Chapter III

Results & Discussion

3. Results and discussion

3.1 Characterization of the properties of the membranes

3.1.1 Morphological characterization of the produced membranes

The fibre diameter and fibre average diameter (in case of ENMCs), and the surface appearance (in case of *Nylaflo* and modified-*Nylaflo*) were analysed through the SEM analysis.

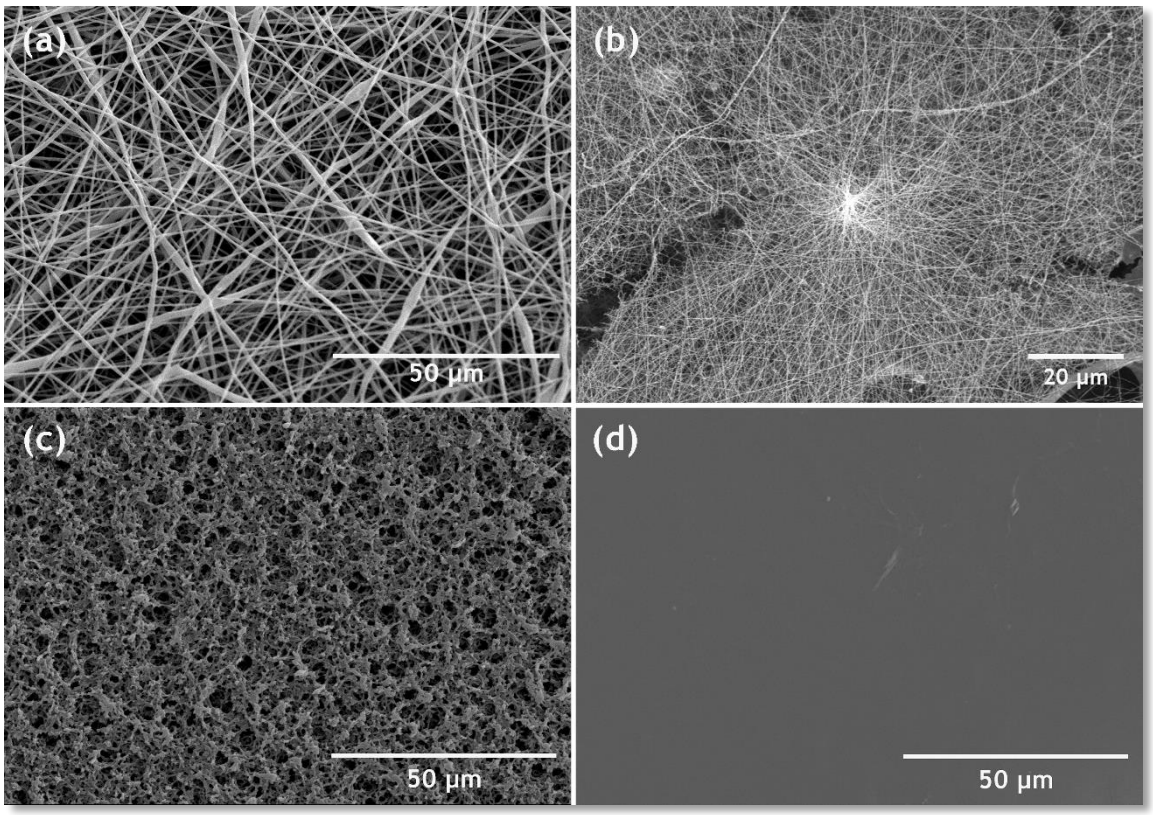

Figure 14 SEM images of PCL ENM (a), PCL ENMC (b), *Nylaflo* (c) and modified-*Nylaflo* (d).

The ENMs produced (figure 14a and b) present a high density of fibres. The ENMs containing the second layer leave even a higher density of nanofibres. The distribution of fibre diameter is shown in Figure 15. The PCL support has nanofibres with different diameters (200 nm – 700 nm) and this range of fibre diameters is ideal to confer a good mechanical support [124], as described by Bosworth *et al.*, PCL meshes presents good mechanical properties [96]. As can be seen, the PCL coated with the *k*-carrageenan presents a higher density of thin fibres (fibres with 100 – 200 nm of diameter) than the PCL uncoated, which contributes to a decrease in the

dimensions of the interstices. The *Nylaflo* membrane surface with/without modification were also analysed (Figure 14c and d). The results revealed that different surface morphologies were obtained after the modification process. As can be observed in Figure 14c the commercial membrane surface showed to be porous, with much larger pores than the nominal 0.22 µm are observed (nominal value given by the manufacturer), indicating a wide pore size distribution. After the modification with agarose the pores could not be observed anymore (Figure 14d).

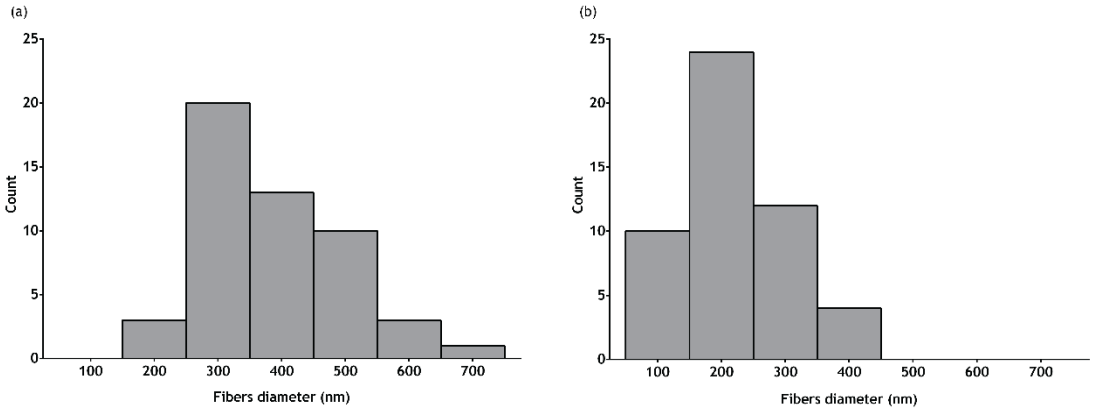

Figure 15 Fibre diameter distribution for the uncoated (a) and coated PCL ENM (b).

SEM image of a cross-section of the modified-*Nylaflo* membrane was also acquired and shows the agarose layer over the surface of the *Nylaflo* membrane (Figure 16). This layer will reduce the porosity and the hydraulic permeability of the *Nylaflo* membrane, conferring characteristics of a UF membrane.

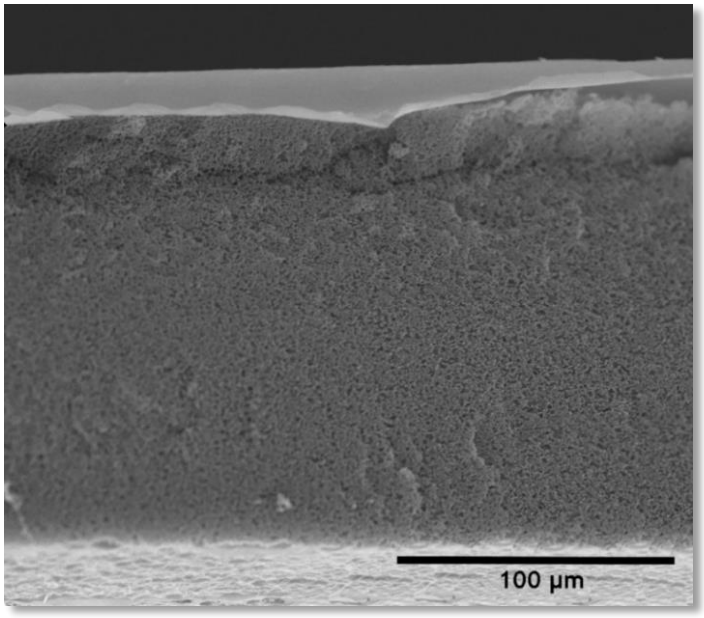

Figure 16 SEM cross-section image of the modified-*Nylaflo* membrane.

The porosity of the membranes, determined gravimetrically, was analysed and the results are presented in Figure 17. As can be seen, the porosity of the ENMCs membranes was similar to the porosity of *Nylaflo* membranes which have been found to be not suitable for the purification of pVAX1-LacZ. Nevertheless, the porosity of the modified-*Nylaflo* membrane decreased to a much lower value, around 40%, than the original *Nylaflo*, about 80%.

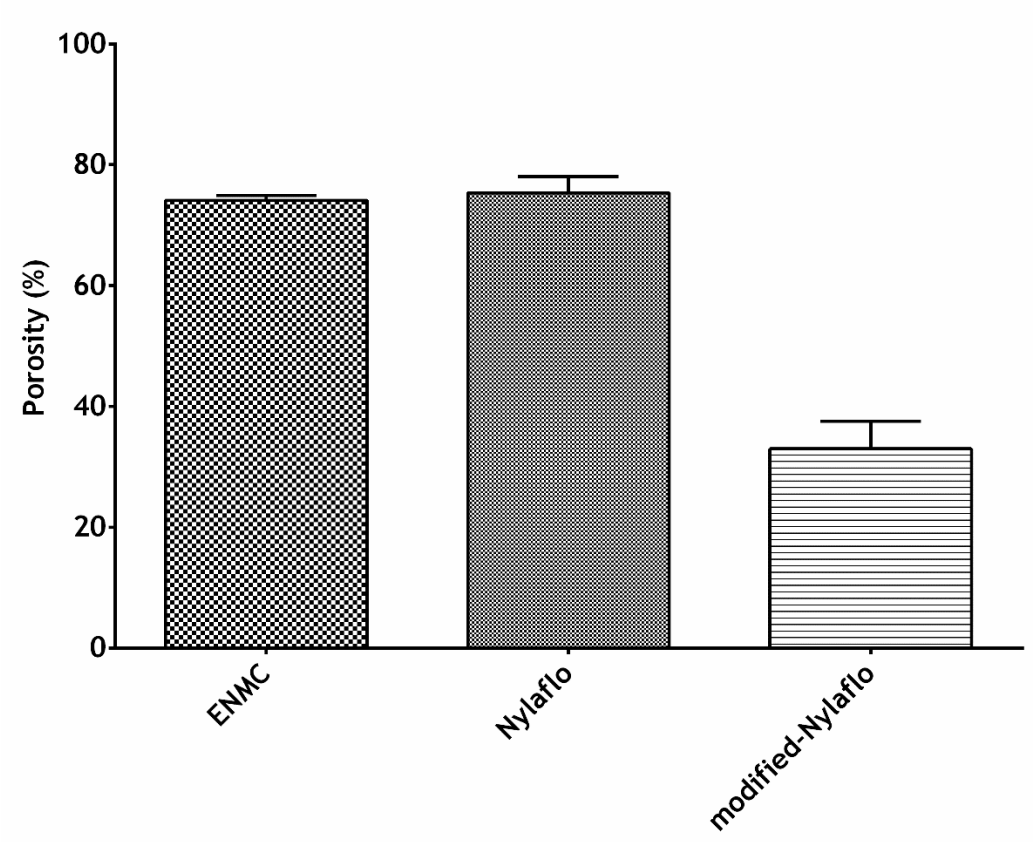

Figure 17 Determination of the porosity of the membranes by immersion in pure ethanol.

3.1.2 Attenuated total reflectance-fourier transform infrared spectroscopy analysis

An ATR-FTIR (Attenuated total reflectance-fourier transform infrared spectroscopy) analysis of the membranes was also carried out to check for the presence of the coating layer on both membranes. Figure 18 shows the ATR-FTIR spectra of PCL, PEO, *k*-carrageenan and PCL/PEO+*k*-carrageenan (polymer coated ENM) and Figure 19 shows the ATR-FTIR spectra of agarose, *Nylaflo* membrane and modified-*Nylaflo*. The spectrum of *k*-carrageenan shows its characteristics absorption bands at 3388 cm^{-1} (-OH stretching) and at 1250 cm^{-1} that belongs to the stretch of S=O group of sulphate group from the anionic polymer [98] (Figure 18a). The spectrum of PEO shows the characteristic bands of $-CH_2$ groups in the region between 2990 cm^{-1} and 2850 cm^{-1} [125] (Figure 18b). In Figure 18c it is presented the spectrum of PCL, which

shows an absorption band between 1750 cm^{-1} and 1740 cm^{-1} due to C=O groups [126]. The spectrum of ENMC (Figure 18d) shows the characteristic peaks of the functional groups of the polymers (PCL, PEO and *k*-carrageenan) used in membrane production, therefore indicating that a thin layer of PEO/*k*-carrageenan was deposited on the PCL support as suggested by the SEM images in section 3.1.1 (Figure 14). Furthermore, an intense peak around 3300 cm^{-1} was observed, due to the over-abundance of OH groups in the coating layer, as previously described in the literature [127, 128].

Figure 19a shows the characteristics peaks of agarose at 3359 cm^{-1} (-OH stretching), 1042 cm^{-1} C-O stretch of sugar molecules, 1636 cm^{-1} (N-H) and 929 cm^{-1} (vibration of C-O-C bridge of 3,6-anydro-L-galactopyranose), in accordance with other reports [129, 130]. The ATR-FTIR spectrum of the *Nylaflo* membrane (Figure 19b) shows the characteristic bands at 3300 cm^{-1}, 2920 cm^{-1}, 2860 cm^{-1} and 1640 cm^{-1} corresponding N-H stretch, CH_2 asymmetric stretch, CH_2 symmetric stretch and amide C=O stretch, respectively [110]. Figure 19c shows that the hydroxyl group peak of agarose at 3359 cm^{-1} is presented in the modified-*Nylaflo*, unlike to that observed in the spectrum of the *Nylaflo* membrane (Figure 19b).

To further verify if the coating is present on the surface of the PCL ENM and the agarose impregnation has occurred, an EDS analysis was also performed.

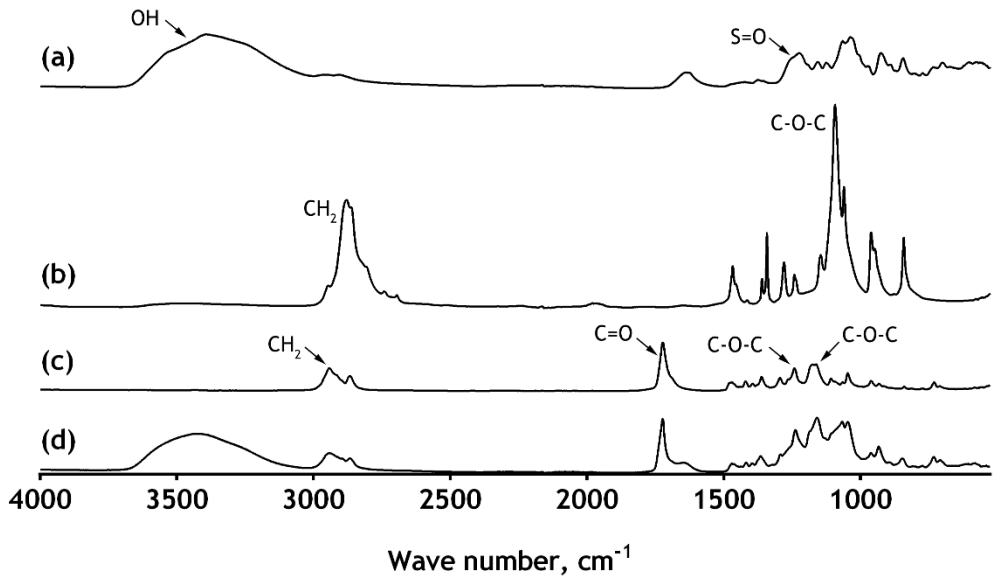

Figure 18 ATR-FTIR spectra of: *k*-carrageenan (a), PEO (b), PCL ENM (c) and PCL ENMC (d).

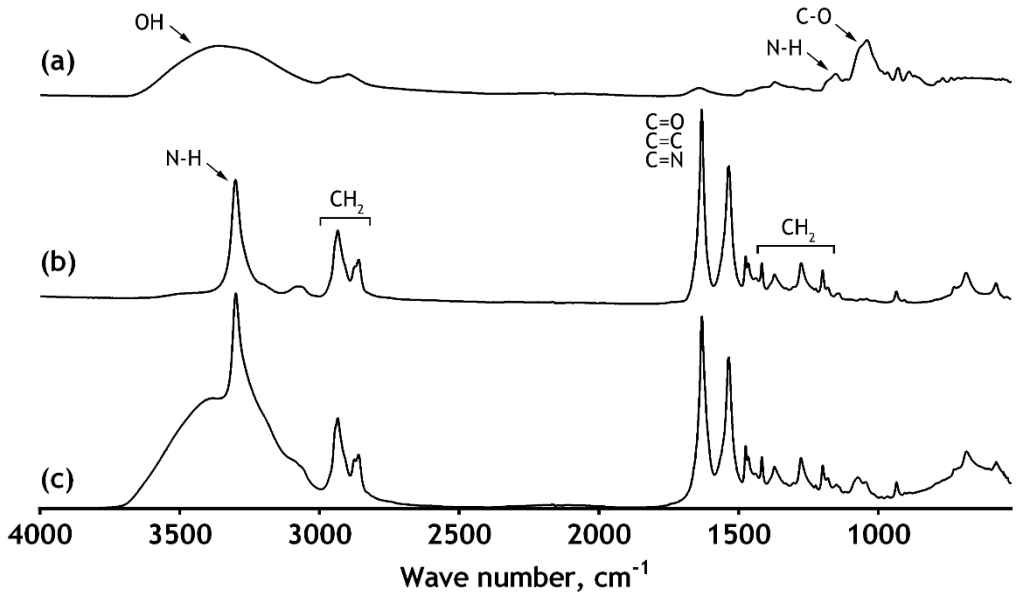

Figure 19 ATR-FTIR spectra of agarose powder (a), *Nylaflo* membrane (b) and modified-*Nylaflo* membrane (c).

The amount of chemical elements at the surface of the PCL ENM and PCL ENM coated membranes (Figure 20) shows that the surface coating of the PCL ENM was achieved due to the increase of the amount of oxygen atoms (characteristic of polyethylene oxid), and the appearance of the sulphur peak (belonging to the negative group of sulphate present in the molecule of *k*-carrageenan) (Table 4)

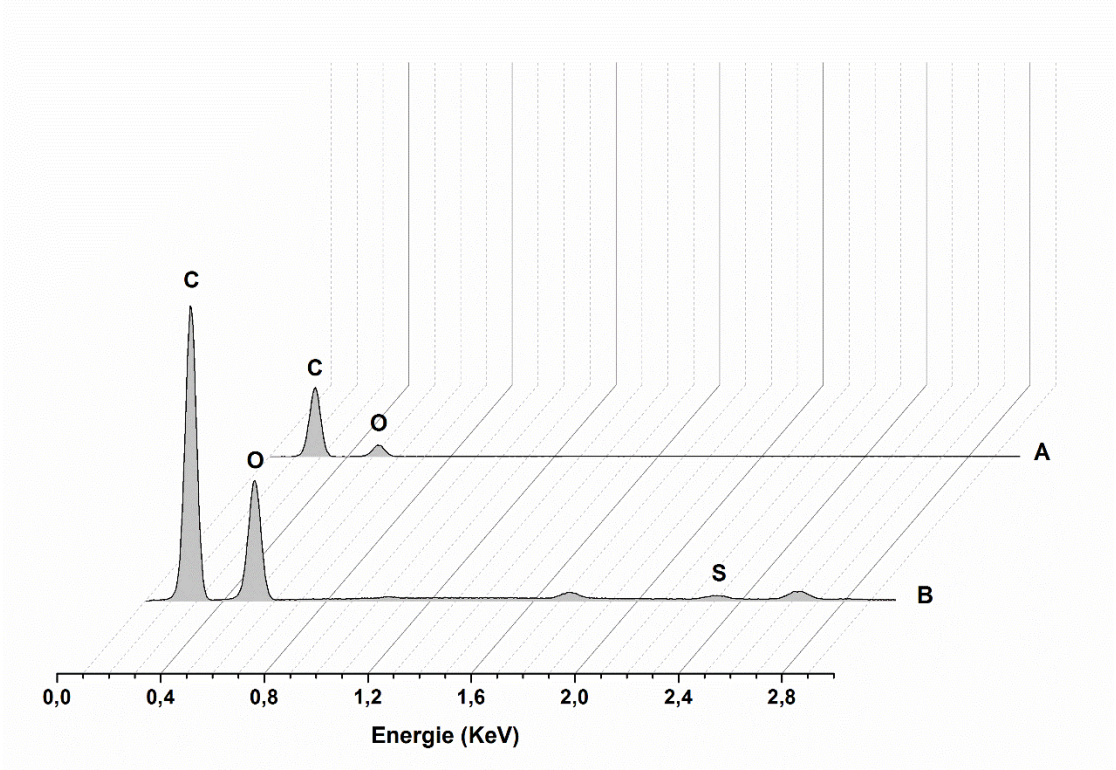

Figure 20 EDS spectra of PCL ENM membrane (a) and PCL ENM coated (b).

Table 4 EDS analysis of the membranes.

Samples	C (at %)	O (at %)	S (at %)
PCL ENM	74.15	25.85	-
PCL ENM coated	62.27	37.61	0.12-

Figure 21 shows the amount of chemical elements at the surface of the unmodified/modified-*Nylaflo* membrane. Herein, it can be concluded that the surface modification was achieved, once the percentage of oxygen elements (characteristic from agarose) was higher for the modified membrane (table 5).

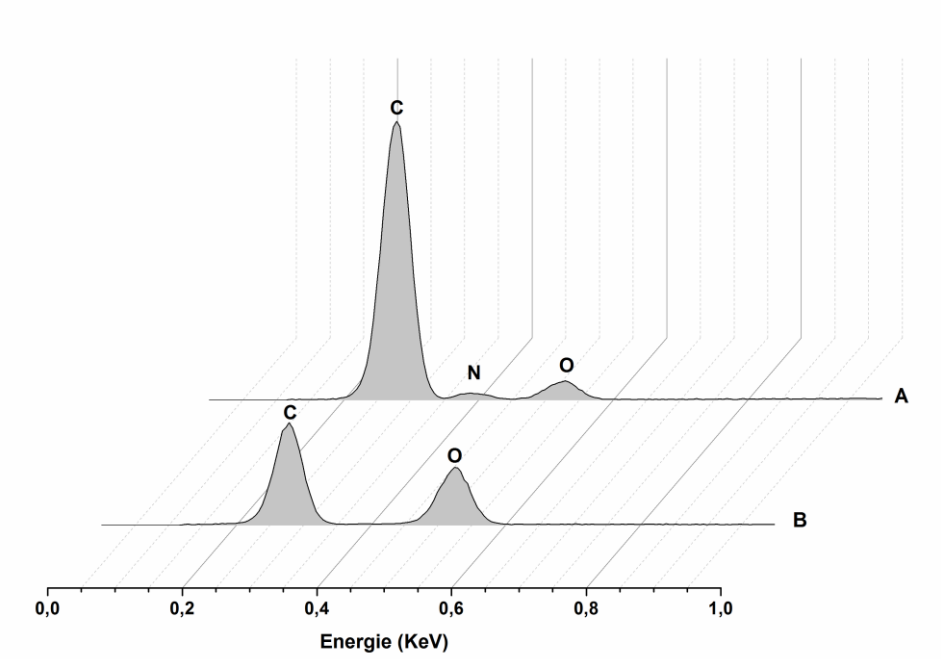

Figure 21 EDS spectra of *Nylaflo* membrane (a) and modified-*Nylaflo* membrane (b).

Table 5 EDS analysis of the membranes.

Samples	C (at %)	O (at %)	N (at %)
Nylaflo	72.06	14.18	13.75
Modified-*Nylaflo*	57.41	42.59	-

3.1.3 Surface properties characterization

Contact angles were determined to evaluate the hydrophobic character of each membrane. This is an important property when considering the filtration of solutions with biomolecules, in fact, it is well-known that hydrophilic membranes generally perform better than hydrophobic, due to the adsorption phenomena of the biomolecules in to the surface of the membrane [131]. As can be seen in Table 6 the uncoated PCL membrane presented a higher contact angle (118.72º), which is indicative of a hydrophobic character. After applying the coat (PEO+*k*-carrageenan) the contact angle decreased to 99.43º, indicating that the membrane became more hydrophilic. The *Nylaflo* membrane showed to be the most hydrophilic, presenting a contact angle of 28.03º for the modified-*Nylaflo* an increase on the contact angle was observed, however the hydrophilic character of the membrane was essentially kept, which is important to prevent the occurrence of fouling phenomena during the purification process, namely due to protein adsorption.

Table 6 Contact angles of the membranes.

Membranes	**Water contact angle**
PCL ENM	118.72º ± 0.73º
PCL ENMC	99.43º ± 0.20º
Nylaflo	28.03º ± 5.40º
Modified-*Nylaflo*	32.68 ± 8.13º

3.2 Membrane filtration studies

3.2.1 Hydraulic permeability

The results obtained in the permeability tests are summarized in figure 22. As can be seen, the coated PCL ENMC and the *Nylaflo* membrane have, approximately, the same L_p values. The modified-*Nylaflo* membrane shows lower L_p values when compared to the original *Nylaflo*. It is worth to note that the L_p values of the modified-*Nylaflo* were the typical of an UF membrane.

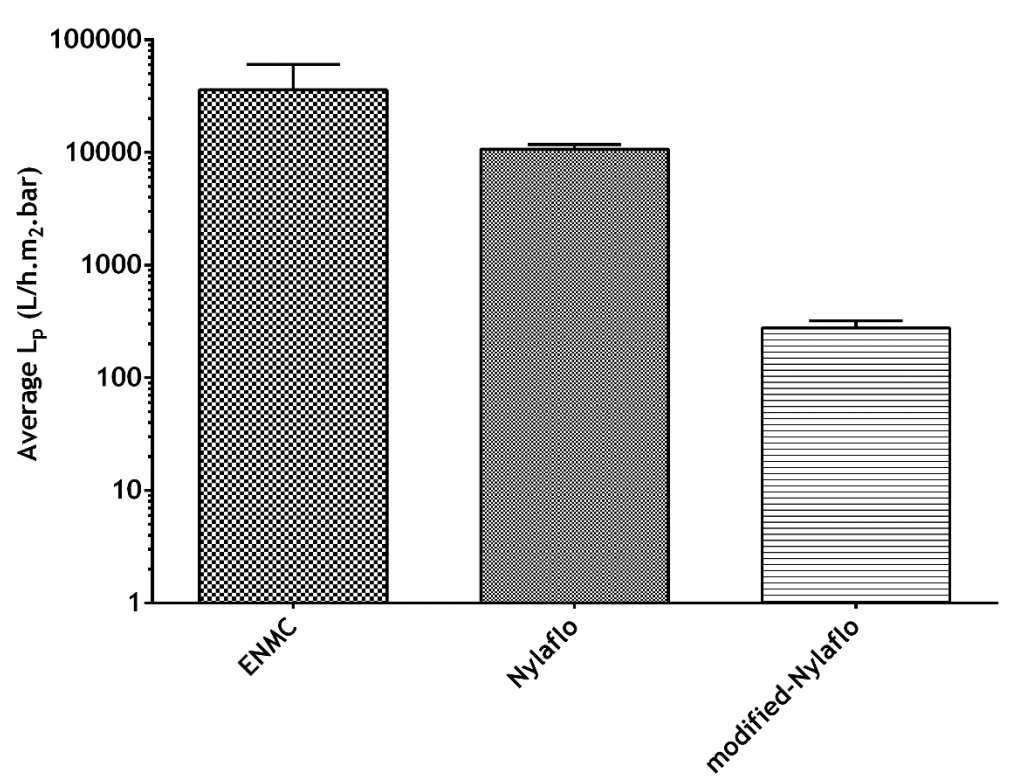

Figure 22 Hydraulic permeability of the different membranes tested, T = 25 ºC.

3.2.2 Estimation of the pore size of the modified-*Nylaflo*

Taking into account the values of hydraulic permeability and the results obtained in the filtration tests (discussed in the section 3.2.3), it was decided to determine only the pore size in the modified-*Nylaflo* membranes.

The pore radius of the modified membranes was estimated from the rejections of reference proteins using the theory of hindered transport of spherical solutes in liquid-filled pores [132], more specifically using the method described as the symmetric pore model, SPM, in [133]. The SPM enables the immediate determination of the membrane pore radius from the intrinsic rejections of a reference solute with a known hydrodynamic radius, r_s, and the L_p of the

membrane [133]. Intrinsic rejections were calculated from the observed rejections, by estimating the mass transfer coefficient of the proteins in the concentration polarization layer, using the correlation proposed by Opong & Zydney [134]. The proteins used in this work and their relevant properties are summarized in Table 7. The observed rejections and the corresponding estimate values of pore radius are indicated in Table 8. The hydraulic permeability of the membranes was measured before and after filtration to confirm the absence of fouling in these tests. The average pore radius obtained was 33 nm, which is substantially lower than the nominal value of the pore radius of the *Nylaflo* commercial membrane, which is 100 nm.

Table 7 Selected properties of the proteins tested.

Protein	Mw (kDa)	r_s (m)	D_s (m^2/s)	Ref
BSA	67	3.55×10^{-9}	6.95×10^{-11}	[135, 136]
γ-globulins	158	5.59×10^{-9}	4.42×10^{-11}	[135, 136]

Table 8 Observed rejections of BSA and γ-globulins at 760 rpm, 25 ºC at the indicated values of transmembrane pressure. Protein concentrations: 0.3 g/L.

Protein	P (bar)	J_v ($L/h.m^2$)	R_{obs}	R_m	r_p (nm)
BSA	0.05	5.3	0.046	0.057	34
	0.10	10	0.054	0.080	28
γ-globulins	0.10	9.8	0.072	0.12	36

3.2.3 Plasmid DNA experiments

Biomolecules separation is important in biology, medicine and chemistry [39, 137]. Herein, pDNA a flexible biomolecule was used in this study. After membrane characterization, the quantification of pDNA rejection was carried out (figure 23 and 24).

As can be seen in Figure 23, when the electrospun membrane (filtration with constant flux) was used, the rejection[4] (R_{obs}) has a tendency to decrease with the increase of the flux (J_v), which is indicative of the occurrence of significant concentration polarization. However, the most

[4] The rejection (R_{obs}) is defined as $1-C_p/C_b$, where C_p is the concentration of the solute (pDNA in this case) in the permeate and C_b is the concentration in the bulk of the feeding solution.

important fact to highlight about these results was the occurrence of pDNA rejection itself, taking into account the very open structure of the produced membranes.

For the modified-*Nylaflo* membrane (filtration with constant pressure), at low fluxes of permeate the membrane presented near 100% of pDNA rejection, which makes it adequated for application in pDNA purification (one cannot say the same about the PCL ENMC membrane). Also, it was again observed that when the flux was increased, the rejection was decreased.

Knowing the r_p value of the modified-*Nylaflo* and the radius of gyration, r_g, of the pDNA molecule, Morão *et al*. [138] had recently shown that one can be accurately estimate through the observed rejections of this type of flexible biomolecules, in the case of several conventional (asymmetric polymeric) ultrafiltration membranes [20, 23, 138]. The model used for the calculations assumes the occurrence of flow induced molecular deformation of the molecular structure of the macromolecules, which leads to their permeation through narrow pores, as a consequence of the permeation flux. The probability of permeation, thus the intrinsic filtering coefficient, can be estimated from the ratio r_g/r_p. In order to estimate observed sieving coefficients it was necessary, also, to estimate the concentration polarization of the macromolecule and for this purpose could be used the correlation obtained by Opong & Zydney [134] as described by Morão *et al*. [138]. Using this model, the theoretical curve (shown in Figure 24) was calculated using r_g = 90 nm; the r_g value depends on the ionic strength of the solution and it was estimated following the method proposed by Morão *et al*. [138]. The observed rejections appeared to be significantly higher than what was predicted, strongly suggesting that the structure of the hydrogel layer (agarose) affected the retention of pDNA molecules, by significantly increasing it. A possible explanation for this phenomena may be that, although the porosity of the modified-*Nylaflo* membranes decreased in respect to the non-modified membrane. The experimental values obtained were still very high, in fact, near 30% of porosity is a very high value for the membrane porosity of an ultrafiltration membrane, considering that conventional ultrafiltration membranes have typical porosities in the range of 2-7% [135, 139]. The effect of the porosity at the membrane surface, which can be identified with the ratio of the pore area to the membrane area, on the rejection of a large flexible molecule like pDNA can be significant, considering that flow-induced deformation is expected to decrease as the porosity increases, due to less suction effects. A similar effect may also explain the unexpectedly high pDNA rejections observed for the PCL ENMS membranes, taking into account the high porosity of these membranes.

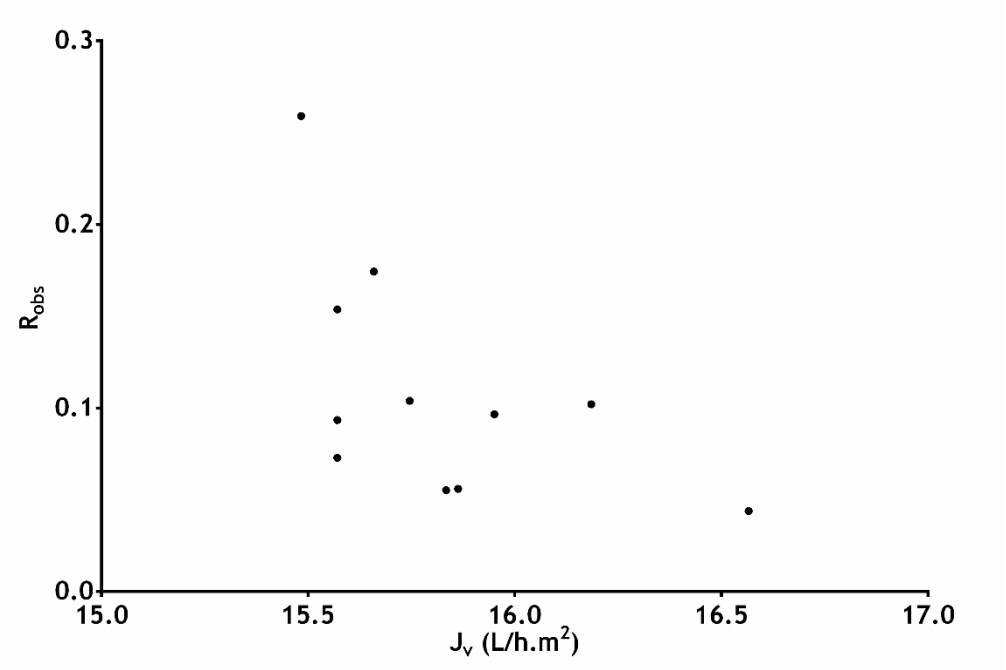

Figure 23 Observed rejections of plasmid *pVax1-LacZ* by the PCL ENMC membrane.

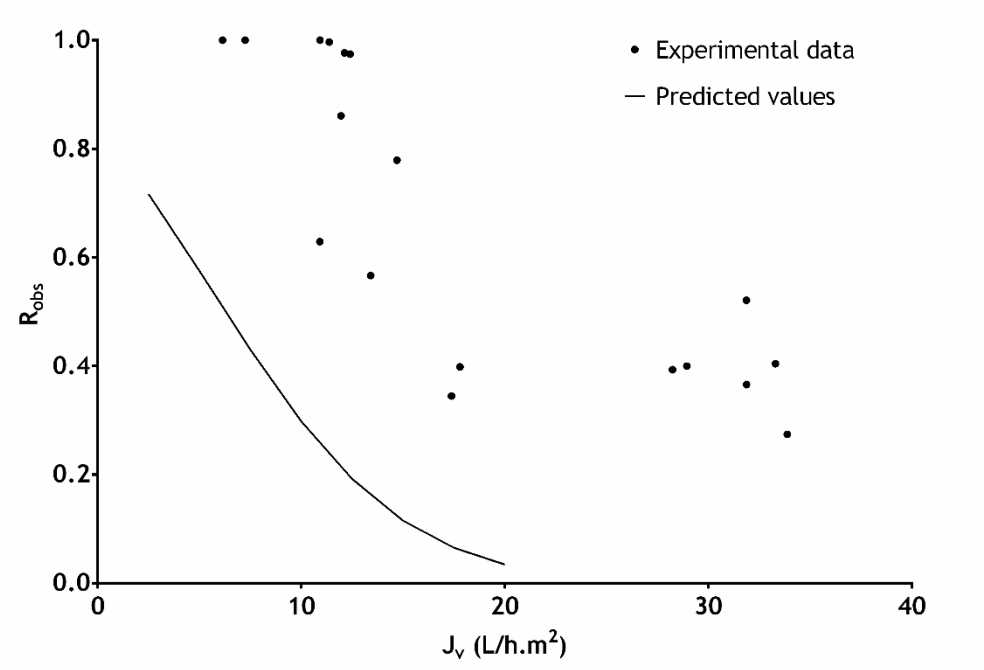

Figure 24 Predicted and observed rejections of plasmid *pVAX1-LacZ* by the modified-*Nylaflo* membrane.

Chapter IV

Conclusion & Future Perspectives

4. Conclusion and future perspectives

In this work two different membranes were produced, an electrospun nanofibre membrane and a modified nylon. The electrospun membrane was produced, by the deposition of a PEO/*k*-carrageenan layer on a PCL support. Both layers (PEO/*k*-carrageenan and PCL) were produced by electrospinning. Electrospun nanofibres that have been previously used in a practical and cost-effective way for the production of polymer scaffolds and also for microfiltration applications were found to be not suitable, however, for pDNA purification since the obtained rejections are not high enough.

The modified-*Nylaflo* membrane presented characteristics of an ultrafiltration membrane, namely in terms of hydraulic permeability and pore size, however with a very high porosity when compared to conventional asymmetric polymeric ultrafiltration membranes. The modified membrane presented 100% of pDNA rejection at low values of flux. Accordingly, these membranes can be used to purify pDNA. This fact and also the simplicity of the modification procedure makes this type of modified membranes potential candidates for being used in practical applications for in pDNA purification.

In future, through the optimization of the electrospinning process of *k*-carrageenan or using other negatively charged polymers, it is possible that UF membranes can be also produced taking into account the importance of the electrical charge of the membrane for pDNA rejection.

Despite the potential shown by modified-*Nylaflo* membranes there were some issues that need to be addressed before considering this work for industrial purposes. The most relevant one is the production process feasibility in large scale which needs to be investigated. Furthermore, pDNA recovery with simultaneous removal of the different contaminants (presented in the process stream before UF) namely RNA removal, needs to be investigated by testing membranes prepared with different agarose concentrations and possibly other hydrogels.

Chapter V

Bibliography

5. Bibliography

1. Schleef, M., *Plasmids for therapy and vaccination*. 2008: John Wiley & Sons.
2. Horn, N.A., et al., *Cancer gene therapy using plasmid DNA: purification of DNA for human clinical trials.* Human Gene Therapy, 1995. **6**(5): p. 565-573.
3. Liu, F., Y. Song, and D. Liu, *Hydrodynamics-based transfection in animals by systemic administration of plasmid DNA.* Gene Ther, 1999. **6**(7): p. 1258-1266.
4. McConkey, S.J., et al., *Enhanced T-cell immunogenicity of plasmid DNA vaccines boosted by recombinant modified vaccinia virus Ankara in humans.* Nature medicine, 2003. **9**(6): p. 729-735.
5. Tang, D.-c., M. DeVit, and S.A. Johnston, *Genetic immunization is a simple method for eliciting an immune response*. Nature, 1992. **356**(6365): p. 152-154.
6. Prather, K.J., et al., *Industrial scale production of plasmid DNA for vaccine and gene therapy: plasmid design, production, and purification.* Enzyme and microbial technology, 2003. **33**(7): p. 865-883.
7. Donnelly, J.J., B. Wahren, and M.A. Liu, *DNA vaccines: progress and challenges.* The Journal of Immunology, 2005. **175**(2): p. 633-639.
8. Ghanem, A., R. Healey, and F.G. Adly, *Current trends in separation of plasmid DNA vaccines: A review.* Analytica chimica acta, 2013. **760**: p. 1-15.
9. Wirth, T., N. Parker, and S. Ylä-Herttuala, *History of gene therapy.* Gene, 2013. **525**(2): p. 162-169.
10. Mountain, A., *Gene therapy: the first decade*. Trends in biotechnology, 2000. **18**(3): p. 119-128.
11. Emery, D.W., *Gene therapy for genetic diseases: On the horizon.* Clinical and Applied Immunology Reviews, 2004. **4**(6): p. 411-422.
12. Liu, M., *DNA vaccines: a review.* Journal of internal medicine, 2003. **253**(4): p. 402-410.
13. Kutzler, M.A. and D.B. Weiner, *DNA vaccines: ready for prime time?* Nature Reviews Genetics, 2008. **9**(10): p. 776-788.
14. Liu, M.A., *DNA vaccines: an historical perspective and view to the future.* Immunological reviews, 2011. **239**(1): p. 62-84.
15. Kahn, D.W., et al., *Purification of plasmid DNA by tangential flow filtration.* Biotechnology and bioengineering, 2000. **69**(1): p. 101-106.

16. Eon-Duval, A., et al., *Removal of RNA impurities by tangential flow filtration in an RNase-free plasmid DNA purification process.* Analytical biochemistry, 2003. **316**(1): p. 66-73.

17. Sousa, F., et al., *Selective purification of supercoiled plasmid DNA from clarified cell lysates with a single histidine-agarose chromatography step.* Biotechnology and applied biochemistry, 2006. **45**(3): p. 131-140.

18. Sousa, F. and J. Queiroz, *Supercoiled plasmid quality assessment by analytical arginine-affinity chromatography.* Journal of Chromatography A, 2011. **1218**(1): p. 124-129.

19. Prazeres, D. and G. Ferreira, *Design of flowsheets for the recovery and purification of plasmids for gene therapy and DNA vaccination.* Chemical Engineering and Processing: Process Intensification, 2004. **43**(5): p. 609-624.

20. Nunes, J.C., et al., *Plasmid DNA recovery from fermentation broths by a combined process of micro-and ultrafiltration: modeling and application.* Journal of Membrane Science, 2012. **415-416**: p. 24-35.

21. Correia, T.R., et al., *A bi-layer electrospun nanofiber membrane for plasmid DNA recovery from fermentation broths.* Separation and Purification Technology, 2013. **112**: p. 20-25.

22. Sun, B., et al., *Large-scale purification of pharmaceutical-grade plasmid DNA using tangential flow filtration and multi-step chromatography.* Journal of bioscience and bioengineering, 2013. **116**(3): p. 281-286.

23. Nunes, J.C., et al., *Plasmid DNA/RNA separation by ultrafiltration: Modeling and application study.* Journal of Membrane Science, 2014. **463**: p. 1-10.

24. De Jong, J., R. Lammertink, and M. Wessling, *Membranes and microfluidics: a review.* Lab on a Chip, 2006. **6**(9): p. 1125-1139.

25. Rathore, A. and A. Shirke, *Recent developments in membrane-based separations in biotechnology processes: review.* Preparative Biochemistry and Biotechnology, 2011. **41**(4): p. 398-421.

26. Plumb, K., *Continuous processing in the pharmaceutical industry: changing the mind set.* Chemical Engineering Research and Design, 2005. **83**(6): p. 730-738.

27. van Reis, R. and A. Zydney, *Bioprocess membrane technology.* Journal of Membrane Science, 2007. **297**(1): p. 16-50.

28. Freitas, S., et al., *Alternatives for the intermediate recovery of plasmid DNA: performance, economic viability and environmental impact.* Biotechnology journal, 2009. **4**(2): p. 265-278.

29. Charcosset, C., *Membrane processes in biotechnology: an overview*. Biotechnology advances, 2006. **24**(5): p. 482-492.

30. Hughes, R., *Industrial membrane separation technology*. 1996: Springer.

31. Van der Bruggen, B., et al., *A review of pressure-driven membrane processes in wastewater treatment and drinking water production*. Environmental progress, 2003. **22**(1): p. 46-56.

32. Baker, R.W., *Membrane technology and applications*. 3rd ed. 2012: John Wiley & Sons.

33. Mulder, M., *Basic principles of membrane technology*. 2nd ed. 1996: Kluwer Academic Pub.

34. Clever, M., et al., *Process water production from river water by ultrafiltration and reverse osmosis*. Desalination, 2000. **131**(1): p. 325-336.

35. Edzwald, J.K., *Water quality & treatment: a handbook on drinking water*. 6th ed. 2011: AWWA and McGraw-Hill Inc.

36. Ferreira Filho, S.S., *Water treatment: principles and design*. 2nd ed. 2005: Montgomery Watson Harsa.

37. *Membrane Filtration*. 1999, National Drinking Water ClearingHouse.

38. Zena-membranes. *Membrane process characteristic*. 2014 [cited 2014 15-08-2014]; Available from: http://www.zena-membranes.cz/index.php/news.

39. Van Reis, R. and A. Zydney, *Membrane separations in biotechnology*. Current Opinion in Biotechnology, 2001. **12**(2): p. 208-211.

40. Wijmans, J. and R. Baker, *The solution-diffusion model: a review*. Journal of membrane science, 1995. **107**(1): p. 1-21.

41. Van Reis, R., et al., *High-performance tangential flow filtration using charged membranes*. Journal of Membrane Science, 1999. **159**(1): p. 133-142.

42. Mehta, A. and A.L. Zydney, *Effect of membrane charge on flow and protein transport during ultrafiltration*. Biotechnology progress, 2006. **22**(2): p. 484-492.

43. Zeman, L.J. and A.L. Zydney, *Microfiltration and ultrafiltration: principles and applications*. 1996: M. Dekker.

44. Hallström, B. and M. Lopez-Leiva, *Description of a rotating ultrafiltration module*. Desalination, 1977. **24**(1): p. 273-279.

45. Chung, K.Y., R. Bates, and G. Belfort, *Dean vortices with wall flux in a curved channel membrane system. IV: Effect of vortices on permeation fluxes of suspensions in microporous membrane*. Journal of membrane science, 1993. **81**(1-2): p. 139-150.

46. Ni, B.-J., B.E. Rittmann, and H.-Q. Yu, *Soluble microbial products and their implications in mixed culture biotechnology*. Trends in biotechnology, 2011. **29**(9): p. 454-463.

47. Yang, Y., et al., *Electrospun fibers with plasmid bFGF polyplex loadings promote skin wound healing in diabetic rats*. Molecular Pharmaceutics, 2011. **9**(1): p. 48-58.

48. Kim, Y.J., M. Ebara, and T. Aoyagi, *A Smart Nanofiber Web That Captures and Releases Cells*. Angewandte Chemie, 2012. **124**(42): p. 10689-10693.

49. Sumitha, M., et al., *Biocompatible and Antibacterial Nanofibrous Poly (ϵ-caprolactone)-Nanosilver Composite Scaffolds for Tissue Engineering Applications*. Journal of Macromolecular Science, Part A, 2012. **49**(2): p. 131-138.

50. Scampicchio, M., et al., *Electrospun Nonwoven Nanofibrous Membranes for Sensors and Biosensors*. Electroanalysis, 2012. **24**(4): p. 719-725.

51. Wu, H., et al., *Electrospun metal nanofiber webs as high-performance transparent electrode*. Nano letters, 2010. **10**(10): p. 4242-4248.

52. Yoon, K., et al., *High flux ultrafiltration membranes based on electrospun nanofibrous PAN scaffolds and chitosan coating*. Polymer, 2006. **47**(7): p. 2434-2441.

53. Barhate, R. and S. Ramakrishna, *Nanofibrous filtering media: filtration problems and solutions from tiny materials*. Journal of Membrane Science, 2007. **296**(1): p. 1-8.

54. Cooper, A., et al., *Chitosan-based nanofibrous membranes for antibacterial filter applications*. Carbohydrate polymers, 2013. **92**(1): p. 254-259.

55. Bhardwaj, N. and S.C. Kundu, *Electrospinning: a fascinating fiber fabrication technique*. Biotechnology Advances, 2010. **28**(3): p. 325-347.

56. Moghe, A. and B. Gupta, *Co-axial Electrospinning for Nanofiber Structures: Preparation and Applications*. Polymer Reviews, 2008. **48**(2): p. 353-377.

57. Yarin, A.L., S. Koombhongse, and D.H. Reneker, *Taylor cone and jetting from liquid droplets in electrospinning of nanofibers*. Journal of Applied Physics, 2001. **90**(9): p. 4836-4846.

58. Fong, H. and D.H. Reneker, *Electrospinning and the formation of nanofibers*. Vol. 6. 2001: Hanser Gardner Publishers.

59. Dzenis, Y.A., *Spinning continuous fibers for nanotechnology*. Science, 2004. **304**: p. 1917–1919.

60. Li, D. and Y. Xia, *Electrospinning of nanofibers: reinventing the wheel?* Advanced materials, 2004. **16**(14): p. 1151-1170.

61. Lyons, J., C. Li, and F. Ko, *Melt-electrospinning part I: processing parameters and geometric properties*. Polymer, 2004. **45**(22): p. 7597-7603.

62. Eggers, J., *Nonlinear dynamics and breakup of free-surface flows*. Reviews of modern physics, 1997. **69**(3): p. 865-930.

63. Fong, H., I. Chun, and D. Reneker, *Beaded nanofibers formed during electrospinning*. Polymer, 1999. **40**(16): p. 4585-4592.

64. McKee, M.G., et al., *Correlations of solution rheology with electrospun fiber formation of linear and branched polyesters*. Macromolecules, 2004. **37**(5): p. 1760-1767.

65. Shenoy, S.L., et al., *Role of chain entanglements on fiber formation during electrospinning of polymer solutions: good solvent, non-specific polymer-polymer interaction limit*. Polymer, 2005. **46**(10): p. 3372-3384.

66. Hohman, M.M., et al., *Electrospinning and electrically forced jets. I. Stability theory*. Physics of Fluids (1994-present), 2001. **13**(8): p. 2201-2220.

67. Zuo, W., et al., *Experimental study on relationship between jet instability and formation of beaded fibers during electrospinning*. Polymer Engineering & Science, 2005. **45**(5): p. 704-709.

68. Huang, Z.-M., et al., *A review on polymer nanofibers by electrospinning and their applications in nanocomposites*. Composites science and technology, 2003. **63**(15): p. 2223-2253.

69. Srinivasan, G. and D.H. Reneker, *Structure and morphology of small diameter electrospun aramid fibers*. Polymer International, 1995. **36**(2): p. 195-201.

70. Demir, M.M., et al., *Electrospinning of polyurethane fibers*. Polymer, 2002. **43**(11): p. 3303-3309.

71. Li, W.J., et al., *Electrospun nanofibrous structure: a novel scaffold for tissue engineering*. Journal of biomedical materials research, 2002. **60**(4): p. 613-621.

72. Megelski, S., et al., *Micro-and nanostructured surface morphology on electrospun polymer fibers*. Macromolecules, 2002. **35**(22): p. 8456-8466.

73. Ayutsede, J., et al., *Regeneration of Bombyx mori silk by electrospinning. Part 3: characterization of electrospun nonwoven mat*. Polymer, 2005. **46**(5): p. 1625-1634.

74. Park, K.E., et al., *Biomimetic nanofibrous scaffolds: preparation and characterization of chitin/silk fibroin blend nanofibers*. International journal of biological macromolecules, 2006. **38**(3): p. 165-173.

75. Huang, L., et al., *Generation of synthetic elastin-mimetic small diameter fibers and fiber networks*. Macromolecules, 2000. **33**(8): p. 2989-2997.

76. Huang, Z.-M., et al., *Electrospinning and mechanical characterization of gelatin nanofibers*. Polymer, 2004. **45**(15): p. 5361-5368.

77. Chew, S.Y., et al., *Mechanical properties of single electrospun drug-encapsulated nanofibres*. Nanotechnology, 2006. **17**(15): p. 3880-3891.

78. Ramakrishna, S., et al., *Electrospun nanofibers: solving global issues*. Materials Today, 2006. **9**(3): p. 40-50.

79. Liang, D., B.S. Hsiao, and B. Chu, *Functional electrospun nanofibrous scaffolds for biomedical applications*. Advanced drug delivery reviews, 2007. **59**(14): p. 1392-1412.

80. Ather, S. and K. Harding, *Wound management and dressings*. Advanced Textiles for Wound Care, 2009: p. 3-19.

81. Thömmes, J. and M.R. Kula, *Membrane chromatography—an integrative concept in the downstream processing of proteins*. Biotechnology progress, 1995. **11**(4): p. 357-367.

82. Klein, E., *Affinity membranes: a 10-year review*. Journal of Membrane Science, 2000. **179**(1): p. 1-27.

83. Gibson, P., H. Schreuder-Gibson, and D. Rivin, *Electrospun fiber mats: transport properties*. AIChE journal, 1999. **45**(1): p. 190-195.

84. Schreuder-Gibson, H., et al., *Protective textile materials based on electrospun nanofibers*. Journal of Advanced Materials, 2002. **34**(3): p. 44-55.

85. Norris, I.D., et al., *Electrostatic fabrication of ultrafine conducting fibers: polyaniline/polyethylene oxide blends*. Synthetic metals, 2000. **114**(2): p. 109-114.

86. Senecal, K., et al., *Photoelectric response from nanofibrous membranes*. Materials Research Society Symposium Proceedings, 2001. **708**: p. 285-292.

87. Ye, P., et al., *Nanofibrous membranes containing reactive groups: Electrospinning from poly (acrylonitrile-co-maleic acid) for lipase immobilization*. Macromolecules, 2006. **39**(3): p. 1041-1045.

88. Jia, H., et al., *Enzyme-carrying polymeric nanofibers prepared via electrospinning for use as unique biocatalysts*. Biotechnology progress, 2002. **18**(5): p. 1027-1032.

89. Yang, Y., J. Wang, and R. Tan, *Immobilization of glucose oxidase on chitosan-SiO_2 gel*. Enzyme and Microbial Technology, 2004. **34**(2): p. 126-131.

90. Kost, J. and R. Langer, *Responsive polymeric delivery systems*. Advanced drug delivery reviews, 2012. **64**: p. 327-341.

91. Verreck, G., et al., *Preparation and characterization of nanofibers containing amorphous drug dispersions generated by electrostatic spinning*. Pharmaceutical research, 2003. **20**(5): p. 810-817.

92. He, W., S.W. Horn, and M.D. Hussain, *Improved bioavailability of orally administered mifepristone from PLGA nanoparticles*. International journal of pharmaceutics, 2007. **334**(1): p. 173-178.

93. Figeys, D. and D. Pinto, *Lab-on-a-chip: a revolution in biological and medical sciences*. Analytical Chemistry, 2000. **72**(9): p. 330 A-335 A.

94. Haiying, L., et al., *Feature of an amperometric ferrocyanide-mediating H2O2 sensor for organic-phase assay based on regenerated silk fibroin as immobilization matrix for peroxidase*. Electrochimica Acta, 1996. **41**(1): p. 77-82.

95. Zhang, Y.-Q., J. Zhu, and R.-A. Gu, *Improved biosensor for glucose based on glucose oxidase-immobilized silk fibroin membrane*. Applied biochemistry and biotechnology, 1998. **75**(2-3): p. 215-233.

96. Bosworth, L.A. and S. Downes, *Physicochemical characterisation of degrading polycaprolactone scaffolds*. Polymer Degradation and Stability, 2010. **95**(12): p. 2269-2276.

97. Qin, X. and D. Wu, *Effect of different solvents on poly (caprolactone)(PCL) electrospun nonwoven membranes*. Journal of thermal analysis and calorimetry, 2012. **107**(3): p. 1007-1013.

98. Jegal, J. and K.H. Lee, *Development of polyion complex membranes for the separation of water-alcohol mixtures. III. Preparation of polyion complex membranes based on the k-carrageenan for the pervaporation separation of water-ethanol*. Journal of applied polymer science, 1996. **60**(8): p. 1177-1183.

99. Lu, J.-W., et al., *Electrospinning of sodium alginate with poly (ethylene oxide)*. Polymer, 2006. **47**(23): p. 8026-8031.

100. Subbiah, T., et al., *Electrospinning of nanofibers*. Journal of Applied Polymer Science, 2005. **96**(2): p. 557-569.

101. Kaur, S., et al., *Plasma-induced graft copolymerization of poly (methacrylic acid) on electrospun poly (vinylidene fluoride) nanofiber membrane*. Langmuir, 2007. **23**(26): p. 13085-13092.

102. Wang, R., et al., *Electrospun nanofibrous membranes for high flux microfiltration*. Journal of Membrane Science, 2012. **392**: p. 167-174.

103. Tang, Z., et al., *Design and fabrication of electrospun polyethersulfone nanofibrous scaffold for high-flux nanofiltration membranes*. Journal of Polymer Science Part B: Polymer Physics, 2009. **47**(22): p. 2288-2300.

104. Tang, Z., et al., *UV-cured poly (vinyl alcohol) ultrafiltration nanofibrous membrane based on electrospun nanofiber scaffolds*. Journal of Membrane Science, 2009. **328**(1): p. 1-5.

105. Liu, Y., et al., *High-flux microfiltration filters based on electrospun polyvinylalcohol nanofibrous membranes*. Polymer, 2012. **54**(2): p. 548-556.

106. Gopal, R., et al., *Electrospun nanofibrous filtration membrane*. Journal of Membrane Science, 2006. **281**(1): p. 581-586.

107. Ritchie, S., et al., *Surface modification of silica-and cellulose-based microfiltration membranes with functional polyamino acids for heavy metal sorption*. Langmuir, 1999. **15**(19): p. 6346-6357.

108. Wang, Y., et al., *Hydrophilic modification of polypropylene microfiltration membranes by ozone-induced graft polymerization*. Journal of Membrane Science, 2000. **169**(2): p. 269-276.

109. Liu, Z.-M., et al., *Surface modification of polypropylene microfiltration membranes by the immobilization of poly (N-vinyl-2-pyrrolidone): a facile plasma approach*. Journal of membrane science, 2005. **249**(1): p. 21-31.

110. Mark, J.E., *Polymer data handbook*. 2nd ed. 2009: Oxford University Press.

111. Johnson, E.M., et al., *Hindered diffusion in agarose gels: test of effective medium model*. Biophysical journal, 1996. **70**(2): p. 1017-1023.

112. Andersson, T., et al., *Agarose-based media for high-resolution gel filtration of biopolymers*. Journal of Chromatography A, 1985. **326**: p. 33-44.

113. Buckley, C.T., et al., *The effect of concentration, thermal history and cell seeding density on the initial mechanical properties of agarose hydrogels*. Journal of the mechanical behavior of biomedical materials, 2009. **2**(5): p. 512-521.

114. Miguel, S.P., et al., *Thermoresponsive chitosan-agarose hydrogel for skin regeneration*. Carbohydrate Polymers, 2014. **111**: p. 366-373.

115. Cao, Z., R.J. Gilbert, and W. He, *Simple Agarose− Chitosan Gel Composite System for Enhanced Neuronal Growth in Three Dimensions*. Biomacromolecules, 2009. **10**(10): p. 2954-2959.

116. Gaspar, V., et al., *Formulation of chitosan–TPP–pDNA nanocapsules for gene therapy applications*. Nanotechnology, 2011. **22**(1): p. 015101-015112.

117. Zargarian, S.S. and V. Haddadi-Asl, *A nanofibrous composite scaffold of PCL/hydroxyapatite-chitosan/PVA prepared by electrospinning*. Iran Polym J, 2010. **19**: p. 457-468.

118. Ma, G., et al., *Electrospun sodium alginate/poly (ethylene oxide) core-shell nanofibers scaffolds potential for tissue engineering applications*. Carbohydrate Polymers, 2012. **87**(1): p. 737-743.

119. Jeong, B., S.W. Kim, and Y.H. Bae, *Thermosensitive sol-gel reversible hydrogels*. Advanced drug delivery reviews, 2002. **54**(1): p. 37-51.

120. Bacsik, Z., J. Mink, and G. Keresztury, *FTIR spectroscopy of the atmosphere. I. Principles and methods.* Applied spectroscopy reviews, 2004. **39**(3): p. 295-363.

121. Fuji, T., et al., *Octacalcium phosphate-precipitated alginate scaffold for bone regeneration.* Tissue Eng Part A, 2009. **15**(11): p. 3525-3535.

122. Nie, H.L. and L.M. Zhu, *Adsorption of papain with Cibacron Blue F3GA carrying chitosan-coated nylon affinity membranes.* Int J Biol Macromol, 2007. **40**(3): p. 261-267.

123. Morão, A., et al., *Development of a model for membrane filtration of long and flexible macromolecules: Application to predict dextran and linear DNA rejections in ultrafiltration.* Journal of Membrane Science, 2009. **336**(1): p. 61-70.

124. Bazargan, A., et al., *A study on the microfiltration behavior of self-supporting electrospun nanofibrous membrane in water using an optical particle counter.* Desalination, 2011. **265**(1): p. 148-152.

125. Ojha, S.S., et al., *Fabrication and characterization of electrospun chitosan nanofibers formed via templating with polyethylene oxide.* Biomacromolecules, 2008. **9**(9): p. 2523-2529.

126. Yang, J., et al., *Preparation of poly epsilon-caprolactone nanoparticles containing magnetite for magnetic drug carrier.* Int J Pharm, 2006. **324**(2): p. 185-190.

127. Tang, C.Y., Y.-N. Kwon, and J.O. Leckie, *Probing the nano-and micro-scales of reverse osmosis membranes—a comprehensive characterization of physiochemical properties of uncoated and coated membranes by XPS, TEM, ATR-FTIR, and streaming potential measurements.* Journal of Membrane Science, 2007. **287**(1): p. 146-156.

128. Tang, C.Y., Y.-N. Kwon, and J.O. Leckie, *Effect of membrane chemistry and coating layer on physiochemical properties of thin film composite polyamide RO and NF membranes: I. FTIR and XPS characterization of polyamide and coating layer chemistry.* Desalination, 2009. **242**(1): p. 149-167.

129. Bhat, S., A. Tripathi, and A. Kumar, *Supermacroprous chitosan-agarose-gelatin cryogels: in vitro characterization and in vivo assessment for cartilage tissue engineering.* Journal of The Royal Society Interface, 2011. **8**(57): p. 540-554.

130. Samiey, B. and F. Ashoori, *Adsorptive removal of methylene blue by agar: effects of NaCl and ethanol.* Chemistry Central Journal, 2012. **6**(1): p. 1-13.

131. Chang, I.-S., S.-O. Bag, and C.-H. Lee, *Effects of membrane fouling on solute rejection during membrane filtration of activated sludge.* Process Biochemistry, 2001. **36**(8): p. 855-860.

132. Deen, W., *Hindered transport of large molecules in liquid-filled pores.* AIChE Journal, 1987. **33**(9): p. 1409-1425.

133. Morão, A., et al., *Characterisation of ultrafiltration and nanofiltration membranes from rejections of neutral reference solutes using a model of asymmetric pores.* Journal of Membrane Science, 2008. **319**(1): p. 64-75.

134. Opong, W.S. and A.L. Zydney, *Diffusive and convective protein transport through asymmetric membranes.* AIChE journal, 1991. **37**(10): p. 1497-1510.

135. Wesselingh, J. and R. Krishna, *Mass transfer in multicomponent mixtures*. 2000: Delft University Press Delft.

136. Yang, K. and Y. Sun, *Structured parallel diffusion model for intraparticle mass transport of proteins to porous adsorbent*. Biochemical Engineering Journal, 2007. **37**(3): p. 298-310.

137. Susanto, H., et al., *Effect of membrane hydrophilization on ultrafiltration performance for biomolecules separation.* Materials Science and Engineering: C, 2012. **32**(7): p. 1759-1766.

138. Morão, A.M., et al., *Ultrafiltration of supercoiled plasmid DNA: modeling and application.* Journal of Membrane Science, 2011. **378**(1): p. 280-289.

139. Wienk, I., T. Van den Boomgaard, and C. Smolders, *The formation of nodular structures in the top layer of ultrafiltration membranes.* Journal of applied polymer science, 1994. **53**(8): p. 1011-1023.

Chapter VI

Appendix

Separation and Purification Technology 112 (2013) 20–25

Contents lists available at SciVerse ScienceDirect

Separation and Purification Technology

journal homepage: www.elsevier.com/locate/seppur

A bi-layer electrospun nanofiber membrane for plasmid DNA recovery from fermentation broths

Tiago R. Correia [a], Bernardo P. Antunes [a], Pedro H. Castilho [a], José C. Nunes [a], Maria T. Pessoa de Amorim [b], Isabel C. Escobar [c], João A. Queiroz [a], Ilídio J. Correia [a,*], António M. Morão [a]

[a] CICS-UBI – Health Sciences Research Center, Faculty of Health Sciences, University of Beira Interior, Covilhã, Portugal
[b] Department of Textile Engineering, University of Minho, 4800-058 Guimarães, Portugal
[c] Department of Chemical and Environmental Engineering, University of Toledo, Toledo, OH 43606, United States

ARTICLE INFO

Article history:
Received 2 February 2013
Received in revised form 28 March 2013
Accepted 29 March 2013
Available online 6 April 2013

Keywords:
Microfiltration
Electrospinning
Bi-layer membrane
Lysate
Plasmid DNA

ABSTRACT

The demanding ever-increasing quantities of highly purified biomolecules by bio-industries, has triggered the development of new, more efficient, purification techniques. The application of membrane-based technologies has become very attractive in this field, for their high throughput capability, simplicity of operation and scale-up.

Herein we report the production of a bi-layer membrane by electrospinning (ES), in which a support of poly ε-caprolactone nanofibers was coated with a polyethylene oxide/sodium alginate layer, and subsequently cross-linked with calcium chloride. The membranes were characterized by SEM, ATR-FTIR, contact angle measurements, and were applied in the recovery process of a plasmid. The results show that membranes retained the suspended solids while allowing the permeation of plasmid DNA, with high recovery yields and improved RNA retention. Moreover, they also showed a very low fouling tendency. To the best of our knowledge it is the first time that ES membranes are applied in this type of bioprocess.

1. Introduction

The development of new separation technologies suitable for the large-scale production of highly purified plasmid DNA (pDNA) for gene therapy applications and the production of DNA vaccines has found increasing interest in the recent years [1–4]. The use of microfiltration and ultrafiltration membranes for pDNA recovery and purification from fermentation broths has been demonstrated as a promising alternative to conventional separation methods, namely those involving precipitation with solvents and centrifugation [5].

Electrospinning is an easy and cheap method of producing nanofibrous materials. These can be obtained from a wide variety of polymers by controlling the solution properties and the processing conditions [6]. The simplicity of this procedure and the wide range of applications found in recent years, including tissue engineering applications, such as bone repair, wound healing and drug delivery carriers [7–9], in sensors and biosensors [10], in electrodes [11] and that of filtration [12–14] are important factors that lead to an increasing interest in developing new types of electrospun nanofiber membranes (ENMs) [15]. Commonly, nanofibers are electrospun into a support or produced in layer by layer arrangements [16,17]. In either case fiber deposition should be always carried out on a support which provides the required mechanical strength to the films produced [16].

In the present study, a poly ε-caprolactone (PCL) support was prepared by a conventional electrospinning process. This polymer was selected based on the good mechanical properties that PCL meshes present [18] and also for being environmentally friendly [19]. A coating based on an electrospun mixture of two polymers, sodium alginate (SA) combined with poly(ethylene) oxide (PEO) was deposited on the support. SA was selected for ENMs coating due to its high hydrophilicity, relatively low cost and the ability of producing small diameter fibers by electrospinning, when mixed with PEO [20]. This asymmetric arrangement of two different layers provides the membrane with adequate mechanical robustness whereas separation selectiveness is regulated predominantly by the ultrathin layer of nanofibers.

The bi-layer membranes produced were characterized in terms of their morphology, hydrophilicity and hydraulic permeability prior to the filtration tests. The performance of the ENMs on the filtration of cell lysates, obtained immediately after the cell lysis step, was evaluated and compared with that of commercial microfiltration membranes. From the best of our knowledge, this is the first time that ENMs are tested in the recovery process of biomolecules from fermentation broths.

* Corresponding author. Address: Av. Infante D. Henrique, 6200-506 Covilhã, Portugal. Tel.: +351 275 329 002; fax: +351 275 329 099.
E-mail address: icorreia@ubi.pt (I.J. Correia).

1383-5866/$ - see front matter © 2013 Elsevier B.V. All rights reserved.
http://dx.doi.org/10.1016/j.seppur.2013.03.049

2. Materials and methods

2.1. Materials

PEO (Mw = 300,000 g/mol), SA (Mw = 120000–190,000 g/mol), PCL (Mw = 80,000 g/mol), calcium chloride (Mw = 110.99 g/mol) were purchased from Sigma–Aldrich (Sin tra, Portugal) as well as Terrific Broth medium for bacterial culture and kanamycin sulfate. P1 buffer (50 mM Tris–HCl, pH = 8.00, 10 mM EDTA and 100 μg/mL of RNase A), P2 buffer (200 mM NaOH and 1% SDS (w/v)) and P3 buffer (3 M of potassium acetate, pH 5.00) were from a Qiagen Plasmid Maxi Kit and Tris–HCl 10 mM (*IZASA*, Portugal). Microfiltration membranes, *Nylaflo* (pore diameter of 0.22 μm *Pall Corporation* and *FSM0.45PP* from *Alfa Laval* (pore diameter of 0.45 μm).

2.2. Methods

2.2.1. Bacterial growth and cell lysis

The plasmid production procedure was adapted from the literature [5,21]. The 6050 bp plasmid pVAX1-LacZ was amplified in a cell culture of *Escherichia coli* DH5α. The fermentation was carried out at 37 °C in 250 mL of Terrific Broth medium, supplemented with 50 μg/mL of kanamycin. Growth was suspended at the late log phase ($OD_{600\_nm} \approx 10–11$) and cells were harvested by centrifugation. Afterwards, pDNA extraction was performed by alkaline lysis using three different buffers (P1, P2 and P3, previously specified). For this procedure 120 g/L (wet weight) of cells were resuspended in 4 mL of P1 buffer. Then, 4 mL of P2 were added to promote cell lysis for 5 min, at room temperature. Finally, P3 buffer at 4 °C was added to neutralize the alkaline solution. A large quantity of suspended solids was obtained upon neutralization and the suspension was kept on ice for 15 min before membrane filtration.

2.2.2. ENMs production process

A conventional electrospinning apparatus was used for ENMs production. The system setup consisted in a high voltage source (*Spellman CZE1000R*, 0–30 kV), a syringe pump (*KDS-100*), a plastic syringe with a stainless steel needle and an aluminum disk connected to a copper collector. PCL was dissolved in acetone (10% w/v), at 50 °C, under constant stirring [22]. Meanwhile, a PEO/SA solution was prepared by mixing 6.75% PEO and 0.5% SA aqueous solutions [23]. The PCL polymer solution was used to produce a support ENM, using a constant flow rate of 3 mL/h and an applied voltage of 15 kV. The distance between needle tip and collector was set at 10 cm [22]. Subsequently, the PEO/SA solution was deposited over the PCL ENM by electrospinning, in the same apparatus, at a constant flow rate of 0.6 mL/h and an applied voltage of 18 kV, thereby obtaining a bi-layer ENM. Finally, the membrane was crosslinked in a calcium chloride solution for 24 h [23]. From the obtained films, membranes disks were cut with suitable size to be used in the filtration cell, using a circular blade.

2.2.3. Membrane filtration tests

These assays were performed in a 10 mL stirred cell (*Amicon*/*Millipore*, model *8010*), according to a procedure previously described in the literature [19]. The membranes to be tested (*Nylaflo*, *FSM0.45PP* or the ENMs) were initially flushed with 20 mL of *Milli-Q* water at a constant pressure of 0.07 bar, to ensure the thorough washing of the membranes. Then, the water permeability (hydraulic permeability) of each membrane was determined by measuring the flow rate, at that pressure. Five permeability measurements were performed with each membrane disk and the average value was considered the initial hydraulic permeability of each membrane disk, L_{p0}.

To perform the filtration of the *E. coli* DH5α lysates the remaining water in the cell was carefully removed and, immediately after that, 10 mL of lysate were introduced in the filtration cell. A continuous diafiltration of the lysate was performed for 1 h, using a 10 mM Tris–HCl (pH = 8.00) buffer at a constant flow rate of 0.5 mL/min. Two peristaltic pumps were used, one for feeding the diafiltration buffer and the other to perform the filtration (by suction). The experimental setup is shown in Fig. 1. Under these conditions, one could estimate that, if no pDNA was adsorbed on the membrane and the membrane rejection was 0, approximately 95% of the pDNA was expected to be recovered in the permeate, while 5% would remain in the cell. It was decided to not try to recover the remaining pDNA to avoid excessive dilution of the whole permeate.

2.2.4. Turbidity measurements

The filtrate was analyzed by UV/Visible Spectroscopy at a wavelength of 600 nm, to determine the amount of suspended solids. A fraction of the alkaline lysate, containing the suspended solids, was transferred to an eppendorf tube and centrifuged at 18,000*g* during 30 min at 4 °C (*Hettich Zentrifugen*, *Mikro 200R*). Then, the absorbance of the supernatant was measured at a wavelength of 600 nm and the value obtained compared with that of the membrane permeates.

2.2.5. Plasmid DNA and RNA quantification

Plasmid DNA and RNA concentrations in lysates, were obtained by hydrophobic interaction chromatography (HIC) [5]. Briefly, a 15 PHE PE column (*Amersham Biosciences – GE Healthcare*) connected to an *AKTA* purifier HPLC System was used. The column was initially equilibrated with 1.5 M $(NH_4)_2SO_4$ in a 10 mM Tris–HCl buffer (pH 8.00). Prior to the injection, the suspended solids in lysates were removed by centrifugation, as described in Section 2.2.4.

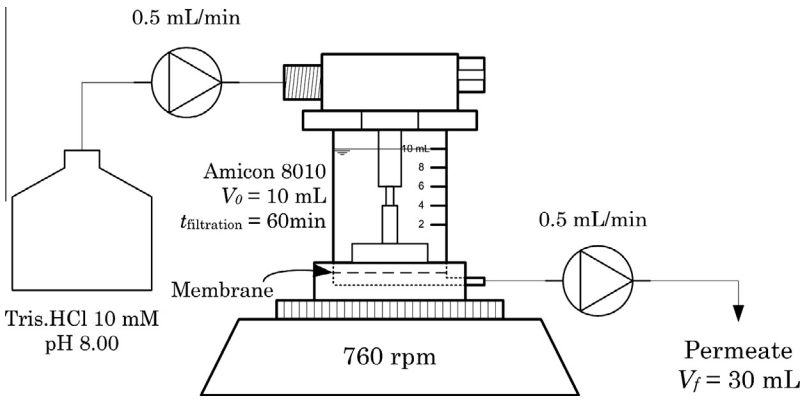

Fig. 1. Experimental set-up used for continuous diafiltrations, showing the two peristaltic pumps and the filtration cell.

Samples from the supernatants were directly injected in the column. The injected volume in each run was 20 μL and the samples were eluted at a constant flow rate of 1 mL/min. Two minutes after the injection, the eluent was instantly changed to 10 mM Tris–HCl buffer (pH = 8.00), in order to elute bounded species. This concentration was maintained for 5 min before the re-equilibration of the column, which was carried out with 1.5 M $(NH_4)_2SO_4$ in a 10 mM Tris–HCl buffer (pH 8.00), in order to prepare the column for the next run. The absorbance of the eluate at 260 nm was monitored. The concentration of pDNA in each sample was calculated from the area of the pDNA peak and a calibration curve, obtained with pure pVAX1-lacZ standard solutions.

The filtration yield, in each test, was calculated as the ratio of the amount of pDNA in the whole collected permeate to the amount of pDNA in the lysate. The RNA removal was calculated as $1 - (V_p C_{RNA,p})/(V_{lys} C_{RNA,lys})$ where $C_{RNA,p}$ is the RNA concentration in the whole collected permeate and $C_{RNA,lys}$ is the RNA concentration in the lysate, V_p is the whole volume of permeate collected and V_{lys} is the volume of lysate processed in each run.

2.2.6. Scanning electron microscopy

The morphology of the membranes was analyzed by scanning electron microscopy (SEM). Samples were air-dried overnight and then mounted on an aluminum board using a double-side adhesive tape and covered with gold using an *Emitech* K550 (London, England) sputter coater. The samples were analyzed using a *Hitachi* S-2700 (Tokyo, Japan) scanning electron microscope operated at an accelerating voltage of 20 kV and at different amplifications [21].

The diameter distribution of the nanofibers in the ENMs was determined from 50 measurements, at least, using *ImageJ* (National Institutes of Health, Bethesda (MD), USA).

2.2.7. Attenuated total reflectance-fourier transform infrared spectroscopy

PEO, SA, PCL and polymer coated ENMs spectra were acquired in the range of 4000–500 cm^{-1}, using a *JASCO* 4200 FTIR spectrophotometer, operating in ATR mode (MKII *GoldenGate*™ Single Reflexion ATR System). Data collection was performed with a 4 cm^{-1} spectral resolution and after 64 scans [24].

2.2.8. Contact angle

Contact angles of the membranes were determined using a *Data Physics Contact Angle System OCAH 200* apparatus, operating in static mode. For each sample, water drops were placed at various locations of the analyzed surface, at room temperature. The reported contact angles are the average of at least three measurements.

2.2.9. Membrane porosity

The surface porosity of the membranes was estimated from SEM images using the image analysis software, *ImageJ*. The total porosity of the membranes was measured through the determination of the amount of ethanol absorbed by wet membranes, after 1 h of immersion in that solvent, using the following equation [25]:

$$P(\%) = \frac{W_2 - W_1}{d_{\text{ethanol}} V_{\text{membrane}}} \times 100 \quad (1)$$

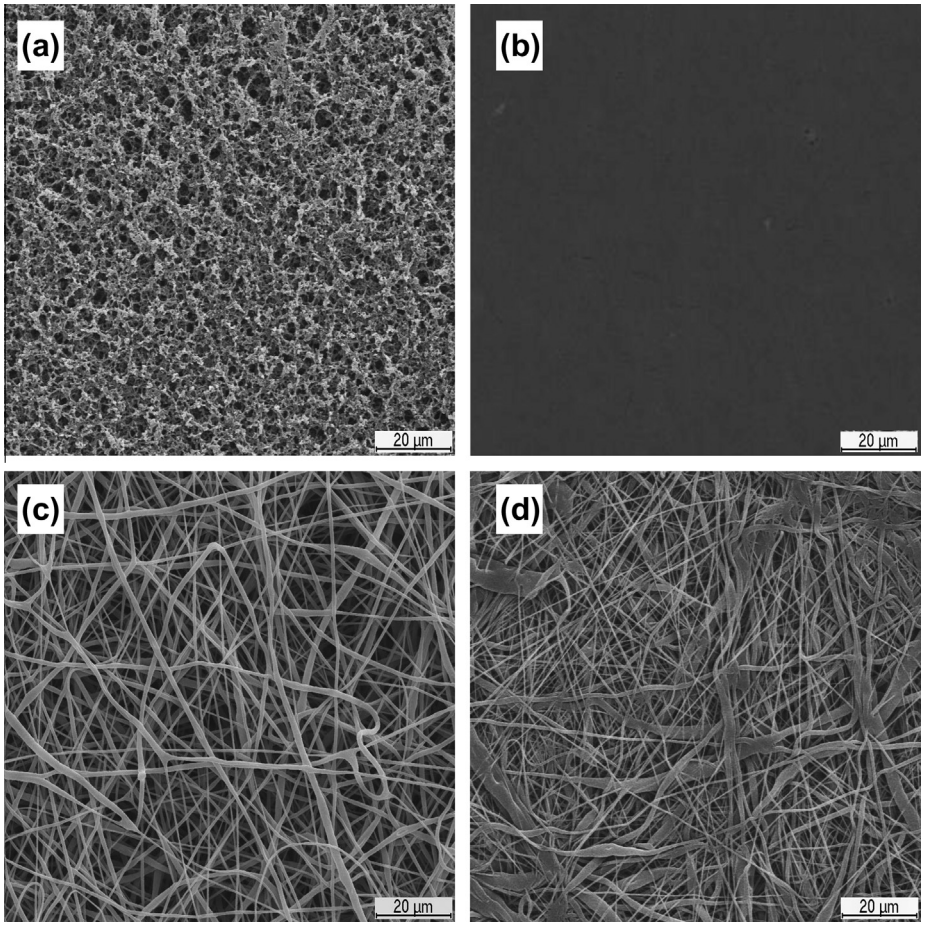

Fig. 2. SEM images. (a) *Nylaflo* 0.22 μm membrane; (b) *FSM0.45PP* 0.45 μm membrane; (c) PCL ENM; and (d) PCL ENMC.

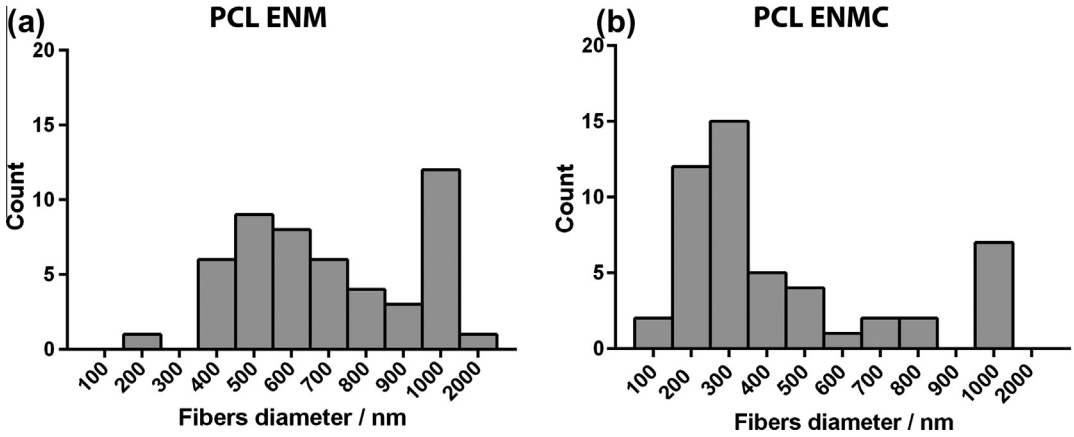

Fig. 3. Fiber diameter distribution for the uncoated and coated PCL ENM.

where W_1 is the weight of the dry membrane and W_2 is the weight of the wet membrane, $d_{ethanol}$ the density of the ethanol at room temperature, and $V_{membrane}$ is the volume of the wet membrane. The latter was determined from the membrane area and by measuring the membrane thickness with a micrometer *Adamel Lhomargy M120* acquired from *Testing Machines Inc*., USA.

3. Results and discussion

3.1. ENMs characterization

The morphology of the membranes, namely in terms of fiber diameter distribution, fiber average diameter and surface porosity was analyzed from SEM images. As can be seen in Fig. 2 the ENMs produced present a high density of deposited fibers, in particular after deposition of the second layer of nanofibers.

Fiber diameter distributions are shown in Fig. 3. The PCL support has nanofibers with different diameters (200 nm – 2 μm) and this range of fiber diameters is adequate for obtaining a good mechanical support [26]. The polymer-coated ENM presents a higher density of thin fibers (i.e., fibers with 200–300 nm of diameter) than the polymer-uncoated ENM (i.e., the PCL support) which contributes to a decrease in the dimensions of the interstices. The number average fiber diameter of the uncoated ENMs can be estimated to be 720 nm and that of the coated membranes to be 430 nm. The commercial microfiltration membranes have typical values of pore diameter for this type of membranes, 0.22 μm and 0.45 μm for the *Nylaflo* and *FSM0.45PP*, respectively (nominal values given by the manufacturers).

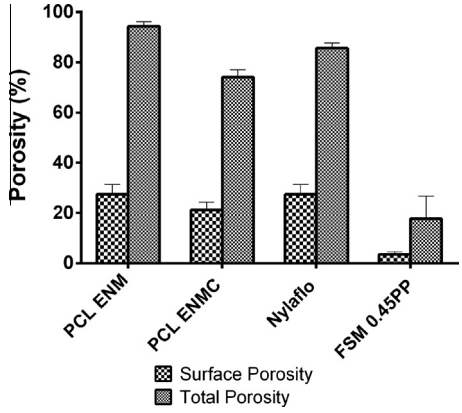

Fig. 4. Surface and total porosity of the ENMs and the commercial microfiltration membranes.

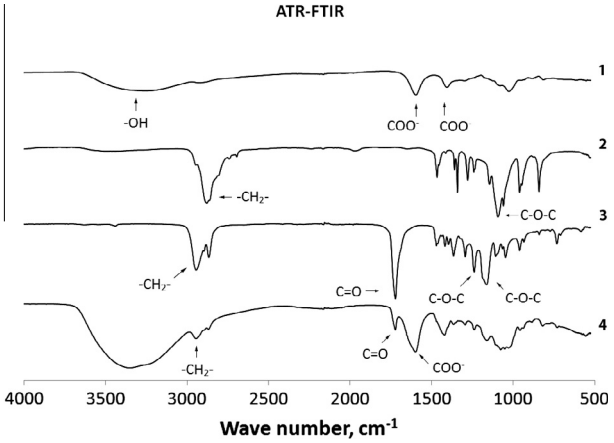

Fig. 5. ATR-FTIR spectra of: (1) SA; (2) PEO; (3) PCL ENM; and (4) PCL ENMC.

The porosity of the membranes is analyzed in Fig. 4. As can be seen, the ENMs have porosities comparable to that of the 0.22 μm *Nylaflo* membranes which have been found to perform very satisfactory in the filtration of lysates from plasmid pVAX1-lacZ fermentation [5]. The porosity of the 0.45 μm membrane used is clearly lower than that of the other membranes studied herein.

An ATR-FTIR analysis of the membranes was also carried out to check for the presence of the coating layer. The ATR-FTIR spectra of SA, PEO, PCL and the PCL/SA ENM (polymer coated ENM) can be seen in Fig. 5. The spectrum of SA shows its characteristic absorption band in the region between 1610 cm^{-1} and 1560 cm^{-1}, which is due to COO^- groups [27] (spectrum 1). The spectrum of PEO (spectrum 2) shows the characteristic bands of —CH2— groups in the region between 2990 cm^{-1} and 2850 cm^{-1} [28]. The third spectrum is that of PCL, which shows an absorption band between 1750 cm^{-1} and 1740 cm^{-1} due to C=O groups [29]. The spectrum of the polymer coated ENM (spectrum 4), shows the characteristic peaks of the functional groups of the polymers used in membrane production, previously mentioned, therefore indicating that a thin layer of PEO/SA was deposited on the PCL support. Moreover, a

Table 1
Contact angles from the FSM, Nylon, uncoated ENM (PCL support) and PCL coated ENM.

Membranes	Water contact angle
FSM0.45PP – 0.45 μm	85.5° ± 3.5°
Nylaflo – 0.22 μm	18.4° ± 0.1°
PCL ENM	104° ± 7°
PCL ENMC	16.8° ± 2.4°

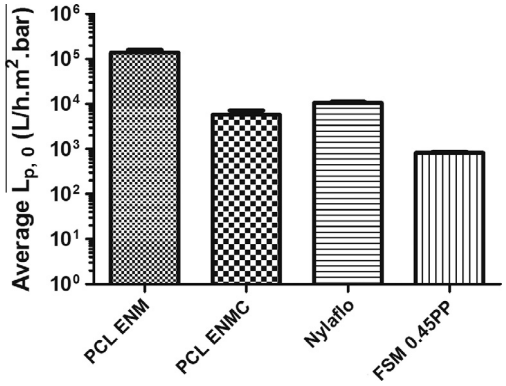

Fig. 6. Water permeability (hydraulic permeability) of the different membranes tested, $T = 25$ °C, before the filtration tests (L_{p0}).

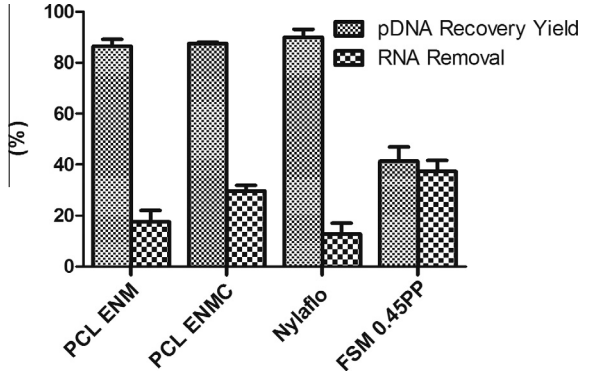

Fig. 7. Filtration yield of the different membranes tested in the filtration of lysates.

much higher intensity peak around 3300 cm^{-1} was observed, due to the over-abundance of —OH groups in the coating layer, as previously described in the literature [30,31].

In order to further characterize the surface properties of the membranes, water contact angles were also determined to evaluate the hydrophilicity of the membranes. This is an important property when considering the filtration of suspensions with high organic load; in fact, it is well-known that hydrophilic membranes generally perform better than hydrophobic due to adsorption phenomena [32]. The obtained contact angles are indicated in Table 1. As can be seen, the uncoated PCL membrane presented a high contact angle of 104°, which is indicative of a hydrophobic character. After coating it with PEO/SA the contact angle decreased to 16.8°, which is a very similar value to that of the *Nylaflo* membrane. The contact angle of the *FSM0.45PP* membrane is also very high, although lower than that of the uncoated PCL ENM. Herein, the filtration tests performed with this membrane aimed to check the effect of the pore size on the permeate turbidity and permeability recover after filtration.

3.2. Membrane filtration studies

3.2.1. Hydraulic permeability

The results obtained in the permeability tests are summarized in Fig. 6. As can be seen, the coated PCL ENM produced have L_{p0} values near 5000 L/h m^2 bar, which are of the same order of magnitude of those found for the *Nylaflo* membrane. The hydraulic permeability of the *FSM0.45PP* is clearly lower, which is possibly due to its lower porosity and also its higher hydrophobicity, as suggested by the results obtained from contact angle measurements.

3.2.2. Microfiltration of lysates

After the cell lysis procedure is completed, using the previously described method, a suspension containing a large quantity of precipitates and cell debris is formed, nearly 2.4 g of suspended solids per gram (wet weight) of cells, as described elsewhere [33]. In respect to solids removal, the coated PCL ENMs and the *Nylaflo* membranes gave identical results. Practically, all solids were removed during the filtration, as can be seen by the turbidity measurements (Table 2). This indicates that both membranes have a similar average pore size. The fact that the uncoated ENMs have a lower solids retention than the coated is in agreement with their higher average fiber diameter, considering that the dimensions of the interstices between fibers becomes smaller as the fiber diameter decreases.

In respect to the process yield, in a previous study, where the same lysis method was used the *Nylaflo* membranes presented high yields for the recovery of pVAX1-lacZ from the obtained lysates [5]. Using both coated and uncoated ENMs, high recovery yields were also obtained herein, as indicated in Fig. 7. In addition, the results also reveal that a significant RNA removal can be achieved using the ENMs, reaching approximately 30% with the PCL coated ENM. It is possible that the structural differences between ENMs and conventional microfiltration membranes can explain the improved selectivity of the ENMs.

With the *FSM0.45PP* membrane the highest RNA removal was found, however, much lower yields are also obtained. The occurrence of severe fouling is likely to be the cause of the higher retention of both pDNA and RNA. In fact, after a few minutes of filtration with this membrane, the permeate pump was unable to impose the predetermined flow of 0.5 mL/min (73 L/h m^2), which is indicative of the intense fouling. In order to accomplish the filtration, the stirred cell had to be connected to a pressurized nitrogen reservoir containing the diafiltration buffer; the applied pressure on the feed was adjusted to 0.5 bar and the permeate pump was disconnected. The permeate flux decreased from 140 L/h m^2 to near 20 L/h m^2 by the end of the diafiltration. Fluxes were determined from the volume of permeate collected as a function of time.

The fouling tendency of the different membranes can be better evaluated by comparing the recovery of hydraulic permeability after filtration, i.e., after replacing the lysate suspension inside the cell with water and then, measuring the water permeability (without subjecting the membranes to any cleaning procedure). The ratio L_p/L_{p0}, is a measure of the tendency of the membranes to foul; the obtained values are shown in Fig. 8. As can be seen, the coated PCL ENMs recovered almost completely their initial permeability upon filtration of the lysates. This indicates that the produced membranes are highly resistant to fouling by the cell debris and other suspended solids present in the lysates.

The differences between the coated and uncoated ENMs should be also pointed out, with the results clearly showing the importance of the PEO/SA layer in preventing membrane fouling. The decrease in the average fiber size may have contributed to a better performance of the coated membranes, by avoiding the accumulation of solids between the fibers, inside the electrospun films. However, the decisive factor affecting membrane performance is more likely to be the increase in hydrophilicity, as it is suggested

Table 2
Turbidity of processed lysates (by centrifugation or microfiltration).

Centrifugation[a]	PCL ENM	PCL ENMC	*Nylaflo*	*FSM0.45PP*
0.002 ± 0.001	0.030 ± 0.001	0.0060 ± 0.0009	0.0065 ± 0.0009	0.024 ± 0.008

[a] As described in Section 2.2.4.

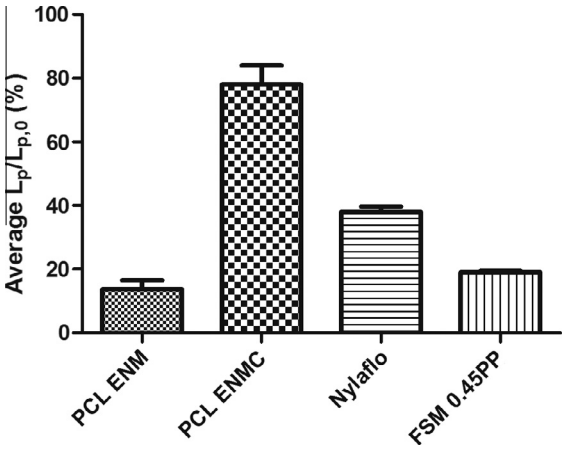

Fig. 8. Permeability recovery of the different membranes tested in the filtration of lysates.

from the fact that both the uncoated ENMs and the *FSM0.45PP* membranes (that had the highest contact angles) present the lowest L_p/L_{p0} values.

4. Conclusion

In this work a bi-layer membrane was produced, by deposition of a PEO/SA layer on a PCL support. Both layers were produced by electrospinning. Electrospun nanofibers that have been previously used in a practical and cost-effective way for the production of polymer scaffolds, are shown here to be also suitable to be used as microfiltration membranes, for processing complex suspensions of solids, with high fouling potential (which is the case of cell lysates). The bi-layer arrangement provided both the selectivity and hydrophilicity required for this application. In fact, the experimental results point out that the bi-layer ENM produced can perform, at least, at the same level as commercial microfiltration membranes, showing a comparable selectivity for retaining the suspended solids while allowing the total permeation of the solute of interest (i.e., the plasmid), with an improved selectivity to retain RNA and an even better resistance to fouling. Moreover, the membranes produced are environmentally friendly due to their known biodegradability.

Acknowledgments

This work was supported by the Portuguese Foundation for Science and Technology (FCT), (PTDC/EME-TME/103375/2008 and PTDC/EBB-BIO/114320/2009). To Ricardo Fradique for helping in the production of the graphical abstract.

References

[1] G.N.M. Ferreira, Chromatographic approaches in the purification of plasmid DNA for therapy and vaccination, Chemical Engineering & Technology 28 (2005) 1285–1294.
[2] M.A. Liu, DNA vaccines: an historical perspective and view to the future, Immunological Reviews 239 (2011) 62–84.
[3] A. Mountain, Gene therapy: the first decade, Trends in Biotechnology 18 (2000) 119–128.
[4] K.J. Prather, S. Sagar, J. Murphy, M. Chartrain, Industrial scale production of plasmid DNA for vaccine and gene therapy: plasmid design, production, and purification, Enzyme and Microbial Technology 33 (2003) 865–883.
[5] J.C. Nunes, A.M. Morão, C. Nunes, M.T. Pessoa de Amorim, I.C. Escobar, J.A. Queiroz, Plasmid DNA recovery from fermentation broths by a combined process of micro- and ultrafiltration: modeling and application, Journal of Membrane Science 415–416 (2012) 24–35.
[6] N. Ashammakhi, A. Ndreu, Y. Yang, H. Ylikauppila, L. Nikkola, Nanofiber-based scaffolds for tissue engineering, European Journal of Plastic Surgery 35 (2012) 135–149.
[7] Y.J. Kim, M. Ebara, T. Aoyagi, A smart nanofiber web that captures and releases cells, Angewandte Chemie International Edition 51 (2012) 10537–10541.
[8] M. Sumitha, K. Shalumon, V. Sreeja, R. Jayakumar, S.V. Nair, D. Menon, Biocompatible and antibacterial nanofibrous poly (ε-caprolactone)–nanosilver composite scaffolds for tissue engineering applications, Journal of Macromolecular Science, Part A 49 (2012) 131–138.
[9] Y. Yang, T. Xia, F. Chen, W. Wei, C. Liu, S. He, X. Li, Electrospun fibers with plasmid bFGF polyplex loadings promote skin wound healing in diabetic rats, Molecular Pharmaceutics 9 (2011) 48–58.
[10] M. Scampicchio, A. Bulbarello, A. Arecchi, M.S. Cosio, S. Benedetti, S. Mannino, Electrospun nonwoven nanofibrous membranes for sensors and biosensors, Electroanalysis 24 (2012) 719–725.
[11] H. Wu, L. Hu, M.W. Rowell, D. Kong, J.J. Cha, J.R. McDonough, J. Zhu, Y. Yang, M.D. McGehee, Y. Cui, Electrospun metal nanofiber webs as high-performance transparent electrode, Nano Letters 10 (2010) 4242–4248.
[12] R. Barhate, S. Ramakrishna, Nanofibrous filtering media: filtration problems and solutions from tiny materials, Journal of Membrane Science 296 (2007) 1–8.
[13] A. Cooper, R. Oldinski, H. Ma, J.D. Bryers, M. Zhang, Chitosan-based nanofibrous membranes for antibacterial filter applications (CARBPOL-D-12-01692-R1, August 26, Carbohydrate Polymers 92 (2012) (2012) 254–259.
[14] K. Yoon, K. Kim, X. Wang, D. Fang, B.S. Hsiao, B. Chu, High flux ultrafiltration membranes based on electrospun nanofibrous PAN scaffolds and chitosan coating, Polymer 47 (2006) 2434–2441.
[15] N. Bhardwaj, S.C. Kundu, Electrospinning: a fascinating fiber fabrication technique, Biotechnology Advances 28 (2010) 325–347.
[16] R. Gopal, S. Kaur, Z. Ma, C. Chan, S. Ramakrishna, T. Matsuura, Electrospun nanofibrous filtration membrane, Journal of Membrane Science 281 (2006) 581–586.
[17] K.C. Krogman, J.L. Lowery, N.S. Zacharia, G.C. Rutledge, P.T. Hammond, Spraying asymmetry into functional membranes layer-by-layer, Nature Materials 8 (2009) 512–518.
[18] L.A. Bosworth, S. Downes, Physicochemical characterisation of degrading polycaprolactone scaffolds, Polymer Degradation and Stability 95 (2010) 2269–2276.
[19] X. Qin, D. Wu, Effect of different solvents on poly(caprolactone) (PCL) electrospun nonwoven membranes, Journal of Thermal Analysis and Calorimetry 107 (2012) 1007–1013.
[20] J.W. Lu, Y.L. Zhu, Z.X. Guo, P. Hu, J. Yu, Electrospinning of sodium alginate with poly (ethylene oxide), Polymer 47 (2006) 8026–8031.
[21] V. Gaspar, F. Sousa, J. Queiroz, I. Correia, Formulation of chitosan–TPP–pDNA nanocapsules for gene therapy applications, Nanotechnology 22 (2010) 015101.
[22] S.S. Zargarian, V. Haddadi-Asl, A nanofibrous composite scaffold of PCL/hydroxyapatite-chitosan/PVA prepared by electrospinning, Iran Polymer Journal 19 (2010) 457–468.
[23] G. Ma, D. Fang, Y. Liu, X. Zhu, J. Nie, Electrospun sodium alginate/poly (ethylene oxide) core–shell nanofibers scaffolds potential for tissue engineering applications, Carbohydrate Polymers 87 (2012) 737–743.
[24] P. Coimbra, P. Alves, T. Valente, R. Santos, I. Correia, P. Ferreira, Sodium hyaluronate/chitosan polyelectrolyte complex scaffolds for dental pulp regeneration: synthesis and characterization, International Journal of Biological Macromolecules 49 (2011) 573–579.
[25] H.L. Nie, L.M. Zhu, Adsorption of papain with Cibacron Blue F3GA carrying chitosan-coated nylon affinity membranes, International Journal of Biological Macromolecules 40 (2007) 261–267.
[26] A. Bazargan, M. Keyanpour-rad, F. Hesari, M.E. Ganji, A study on the microfiltration behavior of self-supporting electrospun nanofibrous membrane in water using an optical particle counter, Desalination 265 (2011) 148–152.
[27] C. Sartori, D.S. Finch, B. Ralph, K. Gilding, Determination of the cation content of alginate thin films by FTIR spectroscopy, Polymer 38 (1997) 43–51.
[28] S.S. Ojha, D.R. Stevens, T.J. Hoffman, K. Stano, R. Klossner, M.C. Scott, W. Krause, L.I. Clarke, R.E. Gorga, Fabrication and characterization of electrospun chitosan nanofibers formed via templating with polyethylene oxide, Biomacromolecules 9 (2008) 2523–2529.
[29] J. Yang, S.B. Park, H.G. Yoon, Y.M. Huh, S. Haam, Preparation of poly ε-caprolactone nanoparticles containing magnetite for magnetic drug carrier, International Journal of Pharmaceutics 324 (2006) 185–190.
[30] C.Y. Tang, Y.N. Kwon, J.O. Leckie, Probing the nano-and micro-scales of reverse osmosis membranes—a comprehensive characterization of physiochemical properties of uncoated and coated membranes by XPS, TEM, ATR-FTIR, and streaming potential measurements, Journal of Membrane Science 287 (2007) 146–156.
[31] C.Y. Tang, Y.N. Kwon, J.O. Leckie, Effect of membrane chemistry and coating layer on physiochemical properties of thin film composite polyamide RO and NF membranes: I. FTIR and XPS characterization of polyamide and coating layer chemistry, Desalination 242 (2009) 149–167.
[32] I.S. Chang, S.O. Bag, C.H. Lee, Effects of membrane fouling on solute rejection during membrane filtration of activated sludge, Process Biochemistry 36 (2001) 855–860.
[33] I. Theodossiou, I. Collins, J. Ward, O. Thomas, P. Dunnill, The processing of a plasmid-based gene from E. coli. Primary recovery by filtration, Bioprocess and Biosystems Engineering 16 (1997) 175–183.